SOUTHEASTERN GEOLOGY

PUBLISHED AT DUKE UNIVERSITY DURHAM, NORTH CAROLINA

VOL. 10 NO. 2 APRIL, 1969

SOUTHEASTERN GEOLOGY

PUBLISHED QUARTERLY

AT

DUKE UNIVERSITY

This journal welcomes original papers on all phases of geology, geophysics, and geochemistry as related to the Southeast. Transmit manuscripts to S. DUNCAN HERON, JR., BOX 6665, COLLEGE STATION, DURHAM, NORTH CAROLINA. Please observe the following:

(1) Type the manuscript with double space lines and submit in duplicate.
(2) Cite references and prepare bibliographic lists in accordance with the method found within the pages of this journal.
(3) Submit line drawings and complex tables as finished copy.
(4) Make certain that all photographs are sharp, clear, and of good contrast.
(5) Stratigraphic terminology should abide by the Code of Stratigraphic Nomenclature (AAPG, v. 45, 1961).

Proofs will not be sent authors unless a request to this effect accompanies the manuscript.

Reprints must be ordered prior to publication. Prices are available upon request.

* * * * * *

Subscriptions to Southeastern Geology are $5.00 per volume. Inquiries should be addressed to WM. J. FURBISH, BUSINESS AND CIRCULATION MANAGER, BOX 6665, COLLEGE STATION, DURHAM NORTH CAROLINA. Make check payable to Southeastern Geology.

SOUTHEASTERN GEOLOGY

Table of Contents

Vol. 10, No. 2

1969

PETROGRAPHY AND GEOCHEMISTRY OF A MAFIC GRANOFELS IN NEWBERRY COUNTY, SOUTH CAROLINA

By

W. G. Libby*
University of British Columbia
Vancouver, B. C., Canada

and

John R. Carpenter
University of South Carolina
Columbia, South Carolina

ABSTRACT

A garnet-clinopyroxene-hornblende-plagioclase-rutile granofels is exposed in two road cuts about 4 miles south of Newberry, Newberry County, South Carolina. Accessories include opaques, sphene, apatite and epidote. The granofels shows discordant contact relationships with the enclosing country rock, a migmatitic quartz-biotite gneiss of the Charlotte Belt.

Much, if not all, of the hornblende and plagioclase is a product of retrogressive alteration of a rock formerly consisting largely or entirely of clinopyroxene, garnet, rutile and opaques. The rock is not an eclogite as indicated by the bulk rock analysis and analyses of garnet and clinopyroxene.

Similarity of the retrogressive plagioclase-hornblende-garnet-epidote assemblage to that of typical mafic rocks of the Charlotte Belt suggests that this assemblage represents the final medium grade regional metamorphism in this area. The earlier garnet-pyroxene-(hornblende?-plagioclase?) assemblage seems to represent an earlier metamorphic event.

INTRODUCTION

A mafic granofels exposed in two road cuts and surrounding woods about 4 miles southwest of Newberry, South Carolina (Figure 1) is of interest as a possible relic, recording conditions prior to the

*Present Address - Department of Geology, San Diego State College, San Diego, California.

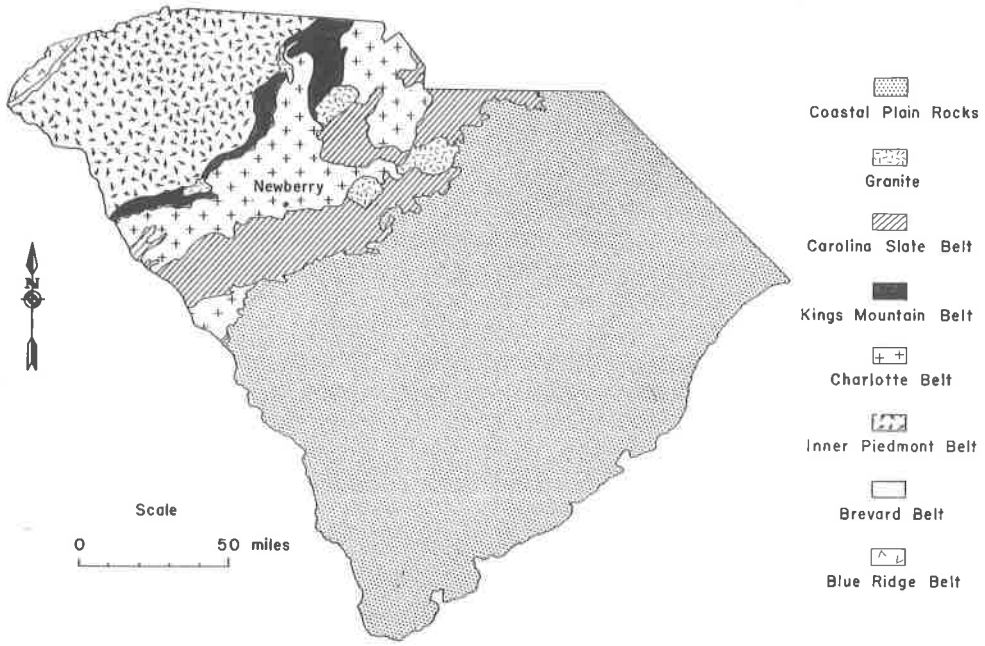

Figure 1. Generalized geologic map of South Carolina showing location of Newberry (after Overstreet and Bell, 1965).

final phase of regional metamorphism that produced the typical gneisses of the Charlotte Belt. The principal minerals are (red) garnet, (green) clinopyroxene, hornblende, plagioclase, rutile, epidote and opaques. Of these the clinopyroxene, garnet, rutile and opaques clearly represent a pre-retrogressive phase, possibly accompanied by some of the hornblende and plagioclase. Hornblende, plagioclase, sphene and epidote represent a later assemblage. Rocks dominated by the garnet-pyroxene assemblage are directionless and grade with increasing hornblende into schistose garnet-epidote amphibolite.

The locality lies within the Charlotte Belt gneiss (McCauley, 1961, Figure 2), more specifically in "Interbedded and migmatized quartz-biotite gneiss of the Charlotte Belt" (McCauley, 1960, Figure 1). A hypersthene-bearing labradorite-biotite-clinopyroxene gabbro, in places uralitized, is exposed in isolated outcrops and float blocks for several miles northwest from the locality. Some of the outcrops of this rock are described by McCauley (1960) in a discussion of the gabbros of the Newberry area. A chlorite-actinolite schist separates the principal locality from a second road cut exposure of mafic granofels about 1/4 mile to the southeast.

MINERALOGY

The proportion of various minerals in the mafic granofels varies greatly between samples within the principal outcrop. Garnet ranges from zero to at least 37 percent, clinopyroxene, from zero to at least 24 percent. Hornblende, plagioclase and opaques seem to be present throughout the outcrop but vary in abundance. Rutile usually is present, especially in those rocks containing clinopyroxene. Epidote and sphene are common. Apatite and carbonate have been observed.

Point counts (1300 to 2100 points per sample) of three clinopyroxene-bearing samples are tabulated (Table 1). The statistical significance of the counts of pyroxene and garnet is not known as the point spacing is 0.5 mm, which is less than the grain diameter of much of the garnet and pyroxene.

The garnet is strictly isotropic and pink in thin section. The grains are roughly equidimensional and only very rarely are partial crystal faces developed. Garnets are generally 1-3 mm in diameter; exceptionally, irregular grains, possibly composite, reach 1 cm in diameter. Irregular fractures commonly have been filled by opaque minerals, hornblende and plagioclase. Evidence for compositional zoning is rare and local, indicated by weak color variation. Isolated, irregularly scattered grains of epidote, hornblende and opaques are included in the garnet. A chemical analysis of the garnet is included in Table 2.

Several clinopyroxene grains were analyzed (Table 3) by J. J. Papike of the U. S. Geological Survey (personal communication, 1968) on an ARL microprobe at the University of Minnesota. The failure of the indicated analyses to total 100.00 percent is due primarily to lack of a sodium analysis. The compositional data were studied by B. J. Morgan of the U. S. Geological Survey (personal communication, 1968) who prepared the information in Table 3. The structural formula (2a)

Table 1. Modal Analyses

Garnet	37.0%	31.2%	31.6%
Clinopyroxene	10.2	18.4	24.1
Hornblende	35.0	35.1	31.2
Plagioclase	7.4	7.5	8.3
Epidote	5.5	0.5	0.1
Rutile	0.3	0.1	0.15
Sphene	0.1	0.3	0.4
Opaques	5.4	7.3	4.15
Apatite	rare	rare	0.1
Zircon	rare		
Hematite	rare		

Table 2.

Garnet Analysis		Number of ions on the basis of 24 oxygens	
SiO_2 (wt. %)	37.5	Si	5.96
TiO_2	0.13	Al	.04
Al_2O_3	21.3	Al	3.94
Fe_2O_3 1/	1.3	Fe^{+3}	.15
FeO 1/	26.74	Ti	.01
MnO	0.40	Fe^{+2}	3.53
MgO	3.6	Mn	.06
CaO	9.0	Mg	.84
Total	99.97	Ca	1.52

In terms of end-member molecules, garnet composition is: Almandite 61.9, Grossularite 20.6, Pyrope 12.0, Andradite 4.1, Spessarite 0.7

Physical Properties

Index of refraction 1.782
Unit cell parameter a = 11.622 Å

1/ FeO and Fe_2O_3 determined wet chemically by C. O. Ingamells, Pennsylvania State University; all other oxide analyses determined spectrochemically by J. R. Carpenter.

is based on the assumption that the entire unanalyzed weight percent is Na_2O, which in fact probably represents a maximum value. Morgan summarizes the clinopyroxene as diopside-hedenbergite (salite) with 10 to 14 percent Tschermak's molecule.

Petrographically, clinopyroxene grains are anhedral and coarse, commonly 3 mm in diameter and in exceptional cases nearly 1 cm in diameter. The pleochroism is: X, pale but distinct green; Z, very pale yellow-green. The pleochroic formula is Y>X>Z. The optic axial angle of non-symplectitic pyroxene measured on the universal stage averages 66° in ten determinations, ranging from 63° to 71°, well above values listed for salite by Deer, Howie and Zussman (1963, Vol. 2, pp. 49-52).

Hornblende is optically similar in all associations though the color varies continuously in some grains and oriented inclusions in pyroxene in rare instances vary in color progressively toward the center of the pyroxene grain. Most hornblende is xenomorphic but subidiomorphic to idiomorphic grains are common. Pleochroism of the hornblende is: X, pale brown; Y, dark olivine-green; Z, dark blue-green.

Table 3.

Clinopyroxene Analysis[1]	(1)	(2)	Number of ions on the basis of 6 oxygens[2]	(1)	(2)
SiO_2 (wt. %)	49.69	49.17	Si	1.896	1.883
FeO[3]	9.04	9.93	Fe^{+2}	.288	.318
CaO	24.13	21.93	Ca	.986	.899
MgO	11.31	10.89	Mg	.643	.621
Al_2O_3	4.33	5.86	Al	.195	.264
	98.50	97.78			

(1) $Ca_{.99}(Mg_{.64}Fe_{.29}Al^{vi}_{.10})_{.94}(Al^{iv}_{.10}Si_{1.90})_{2.0}$

(2) $Ca_{.90}(Mg_{.62}Fe_{.32}Al^{vi}_{.14})_{1.08}(Al^{iv}_{.12}Si_{1.88})_{2.0}$

(2a) $(Na_{.16}Ca_{.89})_{1.05}(Mg_{.61}Fe_{.31}Al^{vi}_{.12})_{1.04}(Al^{iv}_{.14}Si_{1.86})_{2.00}$

Cell dimensions[1]

a = 9.687 Å Errors ± 0.3%
b = 8.858 space group C2/c
c = 5.255
= 106°30' ± 10

1/ Clinopyroxene analysis and cell dimensions from Papike (pers. comm., 1968)
2/ Calculation of cations in unit cell from Morgan (pers. comm., 1968)
3/ Total Fe calculated as FeO

Plagioclase is not quantitatively important in the principal fabric of any of the rocks examined and commonly is absent, particularly in the pyroxene-free schistose rocks. It is abundant in some samples but is interstitial to an amphibole-opaque matrix which is in turn interstitial to coarse clinopyroxene and garnet grains. The plagioclase seems to range from $Ab_{70}An_{30}$ to $Ab_{60}An_{40}$; acute a-normal X':010 extinction angles range from 16° to 22° and the relief is moderate positive.

Rutile is associated with opaque minerals, most commonly in a plagioclase-amphibole matrix interstitial to garnet and pyroxene. Less commonly the rutile is included within garnet. A thin rind of sphene usually coats both opaques and associated rutile.

Epidote (pistacite) forms isolated grains in garnet and rather well defined aggregates of grains in a plagioclase-hornblende matrix interstitial to garnet and clinopyroxene. The epidote constitutes at least as much as 5.5 percent of some samples (Table 1) but is nearly

absent from others. High order interference colors and negative optic sign indicate that the mineral is epidote (s. s.).

Apatite is relatively coarse and not common. Grains commonly are almost 1/2 mm in diameter.

TEXTURES

The most significant textural relationships are those between the plagioclase-hornblende mineral association on the one hand and the clinopyroxene-garnet association on the other. On the basis of texture the various samples can be arranged in a sequence from a rock dominated by garnet and pyroxene with abundant but interstitial hornblende and plagioclase through rocks in which the pyroxene is largely amphibolized, to a rock which is essentially a weakly foliated, quartz-free garnet amphibolite with or without clinopyroxene, epidote, plagioclase or rutile. The most instructive textures are those in rocks with coarsely crystalline, relatively little altered clinopyroxene and garnet. The textures of these rocks will be considered in some detail.

The hornblende has at least three principal modes of occurrence: fine elongate grains, often parallel oriented within pyroxene; medium grains interstitial to garnet and pyroxene, in places forming a crude kelyphitic aggregate with plagioclase; and coarse grains commonly with a core of clinopyroxene and in some instances in optical orientation with the fine hornblende grains with pyroxene. Figure 2 shows the relationship between kelyphitic hornblende and sympletitic pyroxene. The fine and coarse grains probably have a common origin as alteration products of pyroxene whereas the medium grains may be cogenetic with pyroxene and garnet or represent an early stage of the alteration resulting in the fine and coarse grains. Textural differences favor the first interpretation whereas optical similarity, with minor gradational color differences, favor the latter. The pyroxene grains are almost invariably separated from garnet by hornblende or an aggregate of hornblende, plagioclase and opaques. Hornblende tends to be developed against pyroxene and plagioclase against garnet and opaques.

A colorless mineral, probably plagioclase, also is included in clinopyroxene, usually as symplectitic intergrowth in which vermicular rods of plagioclase penetrate the pyroxene host. Non-vermicular plagioclase inclusions are less common than symplectitic plagioclase and usually are associated with hornblende inclusions.

INTERPRETATION

At the earliest stage which can be recognized the rock seems to have been notably rich in garnet and pyroxene. Rutile, opaques and

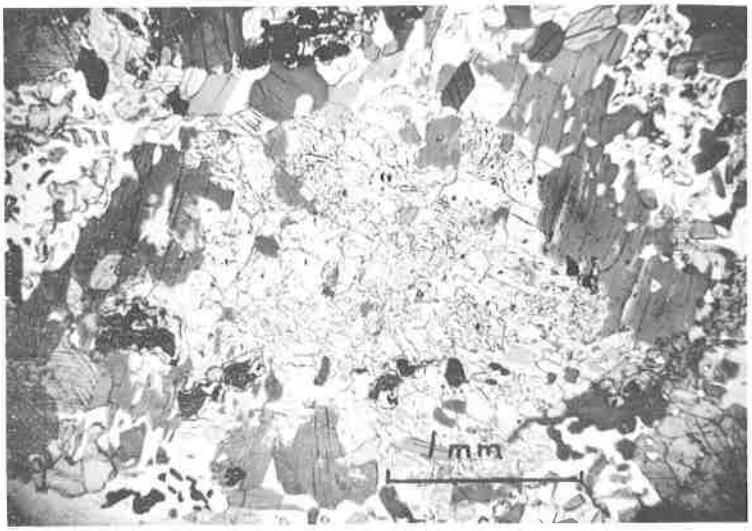

Figure 2. Thin section showing kelyphitic growth of hornblende about symplectitic pyroxene.

apatite probably were accessories. Additional work is presently being carried out by one of us (J. R. Carpenter) in an attempt to determine if the coarse hornblende is compositionally similar to the hornblende found as alteration of pyroxene. It is anticipated that the results of this work will determine if the coarse hornblende was cogenetic with the garnet-pyroxene-rutile assemblage. The likely original assemblage, (red) garnet-(green) clinopyroxene-rutile along with apparently later symplectitic retrogression of pyroxene, coarse xenomorphic texture of the rock, and large optic axial angle of the pyroxene originally led the authors to suspect eclogitic affinities (Libby and Carpenter, in press). The present compositions of garnet and pyroxene do not bear out this interpretation nor does the bulk composition of the rock (Table 4) which is rather different than that of average basalt. Additional field and laboratory studies will be required before we can say with any degree of certainty what the rock was prior to the development of the pyroxene-garnet-rutile assemblage.

The rock is important in that it records part of the petrogenetic history of the region. The retrogressive minerals are similar in assemblage and optic properties to those of other mafic rocks of the Charlotte Belt whereas the alteration of the adjacent gabbro is low grade (chlorite-actinolitic hornblende), suggesting that the mafic granofels predates the gabbro and thus is not a skarn or other metasomatic product of contact metamorphism by the gabbro. The mafic granofels probably is a rock of unusual composition metamorphosed under medium or high grade conditions during or before regional metamorphism of the enclosing Charlotte Belt gneisses and retrogressively

Table 4. Partial Spectrochemical Analysis of Bulk Rocks[1/]

SiO_2	37.0%
TiO_2	2.65
Al_2O_3	11.2
Fe^o [2/]	14.2
MnO	0.16
MgO	7.7
CaO	13.2

1/ Analysis by J. R. Carpenter.
2/ Fe^o = iron as metal, no Fe^{+2} - Fe^{+3} analysis made.

metamorphosed under dynamothermal conditions at medium grade (almandine amphibolite facies) during the regional metamorphic event that produced the gneisses. Knots of pre-retrogressive rock escaped shearing and complete retrogression of the mineral assemblage.

REFERENCES CITED

Deer, W. A., Howie, R. A., and Zussman, J., 1962, Rock-forming minerals: London; Longmans, Green and Co.

Libby, W. G., and Carpenter, John R., Amphibolized eclogite in Newberry County, South Carolina: Geol. Soc. America abstracts for 1967 (Southeastern Sect.). In press.

McCauley, John F., 1960, A preliminary report on the gabbros of Newberry County, South Carolina: Geologic Notes, Div. of Geol., South Carolina State Development Board, v. 4, p. 41-43.

_____, 1961, Relationships between the Carolina Slate Belt and the Charlotte Belt in Newberry County, South Carolina: Geologic Notes, Div. of Geol., South Carolina State Development Board, v. 5, p. 59-66.

Overstreet, W. C., and Henry Bell III, 1965, Crystalline rocks of South Carolina: U. S. Geol. Survey Bull. 1183, 126 p.

p. 307.

THORIUM AND URANIUM IN DETRITAL MONAZITE FROM THE GEORGIA PIEDMONT*

By

William C. Overstreet, Jesse J. Warr, Jr.
and
Amos M. White
U. S. Geological Survey
Washington, D. C.

ABSTRACT

Fifteen samples of detrital monazite from the Georgia Piedmont contain 3.3 to 6.1 percent of ThO_2 and 0.13 to 0.67 percent of U_3O_8, bearing out a previously established relationship of increased thorium content in monazite as the metamorphic grade of the host rock increases. Relations and geologic controls of the amount of uranium in monazite remain unclear; possibly low uranium/thorium ratios associated with high percentages of thorium indicate a granitic source, and high ratios associated with low percentages of thorium indicate paraschist or paragneiss as the source. Further work on this problem is needed.

INTRODUCTION

Fifteen samples of detrital monazite from eight localities in the Piedmont of Georgia were recently analyzed for thorium by J. J. Warr, Jr. The average of these analyses is 4.8 percent of ThO_2 and 0.40 percent of U_3O_8.

This work was done as part of a series of investigations on the distribution and composition of monazite in the Southeastern States begun by J. B. Mertie, Jr., U. S. Geological Survey, in 1945 (Mertie, 1953, 1955, 1956, and 1957; Overstreet, Theobald, and Whitlow, 1959; Overstreet, 1960, 1967; Overstreet, Yates, and Griffitts, 1963).

Only one analysis showing thorium and uranium in Georgia monazite has previously been published (Mertie, 1953), although monazite was known in Georgia gold placers as early as 1888 (Engineering and Mining Journal, 1888). This monazite, from the Flint River, Spalding County, contained 4.42 percent of ThO_2 and 0.26 percent of U_3O_8. An earlier analysis, showing 4 percent ThO_2 but not giving uranium, was published by Pratt (1916) for detrital monazite from a gold placer in the extreme northern part of the State.

*Publication authorized by the Director, U. S. Geological Survey.

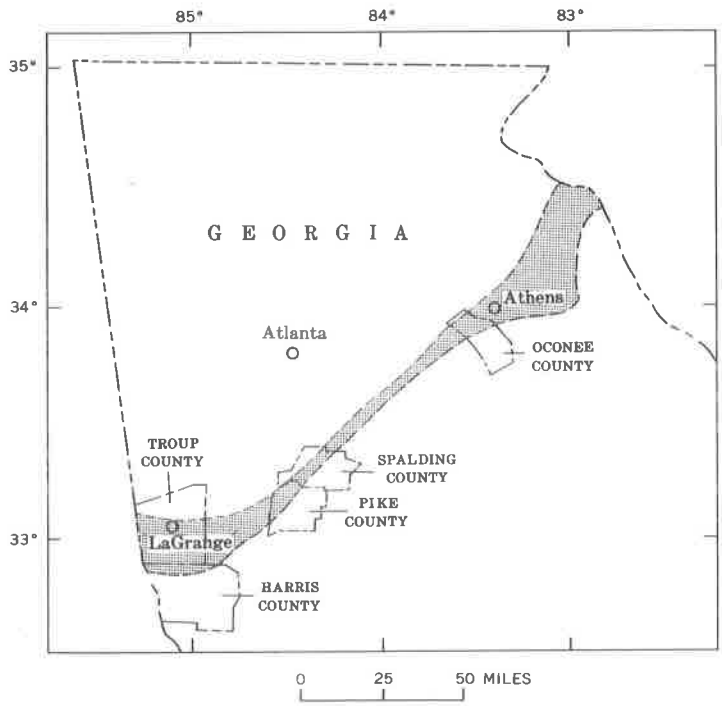

Figure 1. Index map of northern Georgia showing location of the three areas where detrital monazite was collected. The western monazite belt is shaded. Outline of the belt is modified from Mertie, 1953, pl. 1.

Lack of analyses prevented a test of the relation between the regional grades of metamorphism of the host rocks of monazite in Georgia and the abundance of thorium in the monazite. The lack of analyses of monazite from fluviatile placers is also a handicap to an evaluation of Georgia placers as commercial sources for thorium. These 15 new analyses contribute information to both problems.

LOCATION AND GEOLOGIC RELATIONS OF THE SAMPLES

The monazite came from three areas in the western monazite belt in Georgia (Mertie, 1953) (Figure 1 and Table 1): (1) Oconee County (Figure 2), (2) Spalding County and Pike County (Figure 3), (3) Harris County and Troup County (Figure 4). The monazite is detrital. It is inferred to be derived locally from weathered rocks in the drainage basins of the streams from which it was taken.

Table 1. Location of Samples of Detrital Monazite and Description of Source Rocks in Oconee, Spalding, Pike, Harris, and Troup Counties, Georgia

Sample Number	Location and Material Sampled	Source
	Oconee County (Fig. 2)	
52-PK-177	Riffle gravel, Barber Creek 2.5 miles upstream from junction with McNutt Creek	Biotite schist and biotite gneiss in migmatite complex of dominant staurolite-kyanite subfacies locally reaching sillimanite-almandine subfacies (Parizek, 1953; 1955).
52-PK-208	Riffle gravel, McNutt Creek northern headwater tributary 1.6 miles upstream from Clarke County line	do.
52-PK-261	Riffle gravel, west tributary to Rose Creek 3.3 miles upstream from county line	Granite and sillimanite-biotite schist and isofacial rocks dominantly of sillimanite-almandine subfacies (P. K. Theobold, Jr., written commun., 1952).
	Spalding County (Fig. 3)	
52-DC-790	Riffle gravel, Flat Creek 0.8 mile upstream from junction with Flint River	Biotite granite intrusive into biotite schist, staurolite-kyanite subfacies (D. W. Caldwell, written communication, 1952).
	Pike County (Fig. 3)	
52-DC-791	Riffle sand, westernmost major southern tributary to Flat Creek 1 mile south of county line and 3 miles from Flint River	Biotite granite intrusive into biotite gneiss and biotite schist, staurolite-kyanite subfacies (D. W. Caldwell, written communication, 1952; Stose and Smith, 1939).
	Harris County (Fig. 4)	
52-DC-778	Riffle gravel, eastern tributary to Flat Shoals Creek entering 1.3 miles upstream from Chattahoochee River, sample located 2.8 miles upstream from river	Biotite schist and biotite gneiss, staurolite-kyanite subfacies and lower metamorphic grade (D. W. Caldwell, written communication, 1952; Hewett and Crickmay, 1937).
	Troup County (Fig. 4)	
52-DC-768	Riffle gravel, southern tributary to Flat Shoals Creek 10.2 miles due south of La Grange	Biotite schist and biotite gneiss, isofacial with staurolite-kyanite subfacies but lack kyanite (D. W. Caldwell, written communication, 1952).
52-DC-710	Riffle gravel, Yellowjacket Creek 1.2 miles upstream from Chattahoochee River	Biotite schist and Snelson Granite, granite dominant; staurolite-kyanite subfacies or lower metamorphic facies (D. W. Caldwell, written communication, 1952).

52-PK series collected by P. K. Theobald, Jr., and 52-DC series collected by D. W. Caldwell, U. S. Geological Survey.

ABUNDANCE OF THORIUM AND URANIUM

Determinations of the abundances of thorium and uranium in the 15 samples of monazite from Georgia was part of a broader program of analysis which included more than 100 samples of monazite from the Carolinas. Duplicate analyses for thorium were made on every tenth sample of the whole lot using a second analytical procedure. The results of the analyses of the Carolina monazites have not been described.

Preparation of the Monazite

The detrital monazite used for these analyses was obtained by screening and panning 40-pound samples of riffle gravel and riffle sand

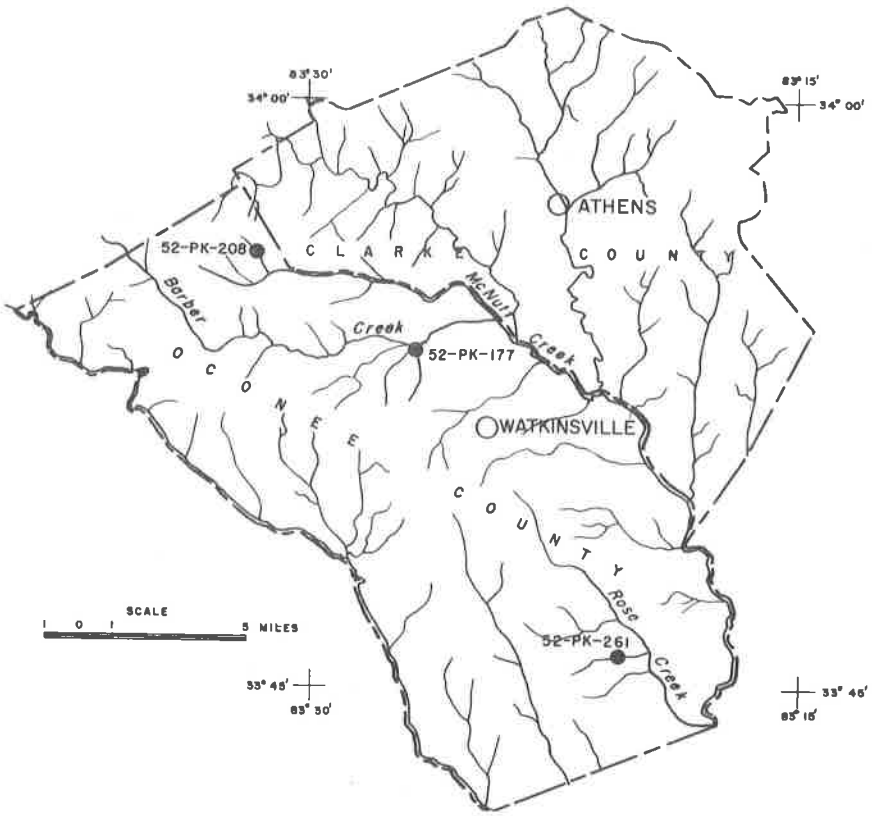

Figure 2. Index map showing locations of analyzed samples of detrital monazite in Oconee County, Georgia.

from the streams. About 300 milligrams of monazite was hand picked from each concentrate, and the monazite separate was tested under unfiltered ultraviolet light by the method of Murata and Bastron (1956) to be certain that xenotime was absent.

Methods of Analysis

Thorium was determined spectrophotometrically with thoron (Fletcher and others, 1957). Checks of the thorium determinations were made by another spectrophotometric method using arsenazo III as the reagent (May and Jenkins, 1965). Uranium was determined fluorometrically after isolation of the uranium and fusing with a flux containing NaF (Grimaldi and others, 1954).

Results

The results of the analyses, given as ThO_2 and U_3O_8, are shown in Table 2.

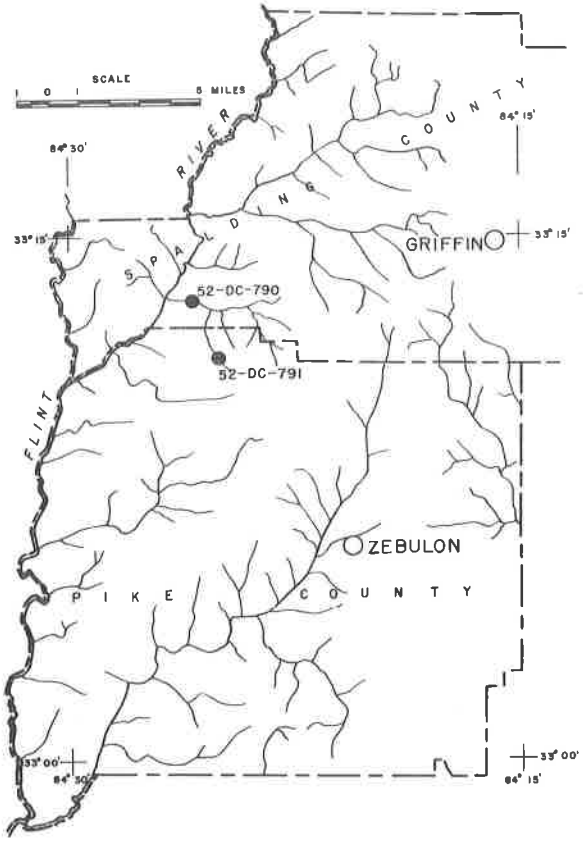

Figure 3. Index map showing locations of analyzed samples of detrital monazite in Spalding and Pike Counties, Georgia.

INTERPRETATION OF THE COMPOSITION

Thorium

Relation to grain size. Grain size of monazite tends to be coarser in the handpicked separate than in the concentrate as a whole, because large grains are easier to pick than small grains. It has previously been shown that monazite grains from pegmatite tend to be coarser than monazite grains from schist and gneiss in the same area (Overstreet, Yates, and Griffitts, 1963), and that monazite from pegmatite tends to be somewhat richer in thorium than monazite from wallrock schist and gneiss (Overstreet, 1967, p. 202-203). Therefore, if pegmatite was an important factor as a source for monazite in these areas, and if the coarser grains in the analyzed monazite separates were mainly from pegmatite, then the possibility exists that the amounts

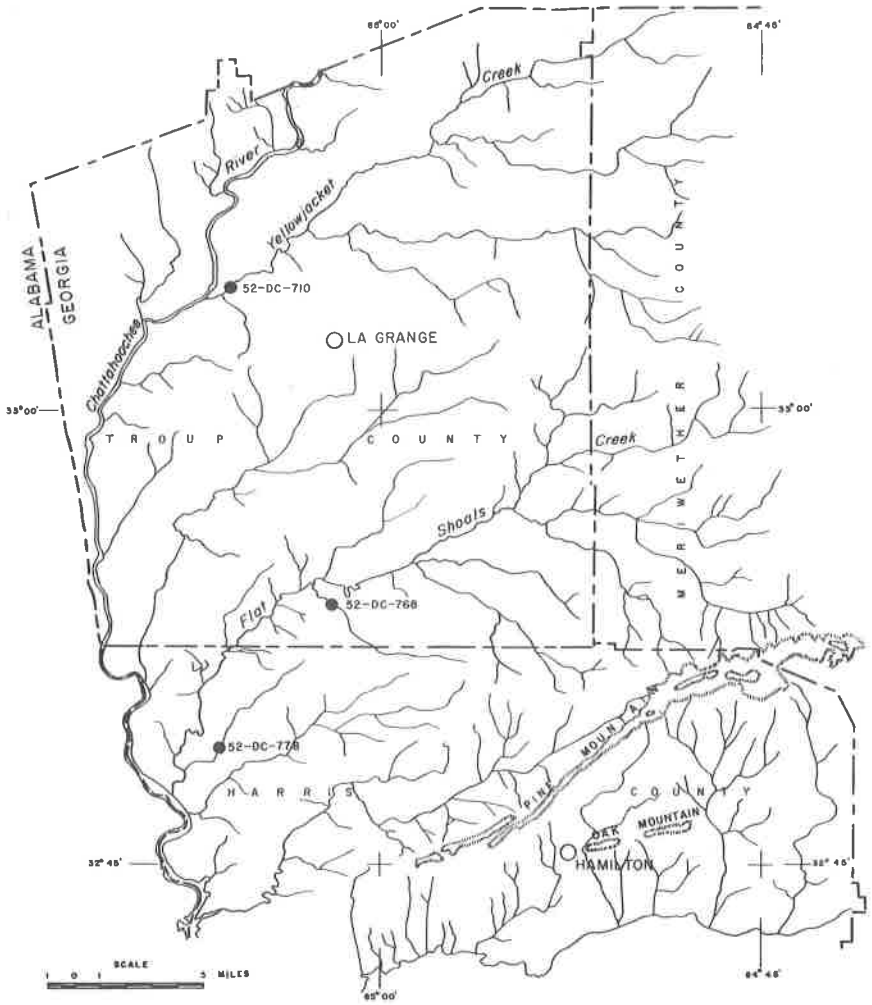

Figure 4. Index map showing locations of analyzed samples of detrital monazite in Harris and Troup Counties, Georgia

of thorium in the handpicked monazite separates might be biased in the high-thorium direction. To test this possibility the monazite separates were divided for analysis into +40-mesh and -40-mesh fractions.

The five samples coarser than 40 mesh have an average of 4.7 percent ThO_2, and the 10 samples finer than 40 mesh have an average of 4.8 percent ThO_2 (Table 2). In the five pairs of samples giving coarser and finer grains for analysis (52-PK-177A and B, 52-PK-208A and B, 52-PK-261A and B, 52-DC-791A and B, 52-DC-778A and B), the coarse-grained fractions are richer in thoria by only 0.1 percent in three samples and leaner by a greater range in two samples. Thus, in

Table 2. Abundances of ThO_2 and U_3O_8 in Detrital Monazite from the Georgia Piedmont.
[Analyst, J. J. Warr, Jr., U. S. Geological Survey]

Sample Number	Size Fraction (mesh)	ThO_2 (percent)	U_3O_8 (percent)	U_3O_8/ThO_2
		Oconee County		
52-PK-177A	-40	4.0	0.47	0.11
52-PK-177B	+40	3.3	.50	.15
52-PK-208A	-40	4.7	.67	.14
52-PK-208B	+40	4.9	.57	.11
52-PK-261A	-40	6.0	.44	.07
52-PK-261B	+40	6.1	.43	.07
		Spalding County and Pike County		
52-DC-790A	-40	5.4	.24	.04
52-DC-791A1	-60	5.6	.16	.03
52-DC-791A2	-60+80	5.7	.17	.03
52-DC-791A3	-80	5.6	.18	.03
52-DC-791B	+40	5.5	.13	.02
		Harris County and Troup County		
52-DC-778A	-40	3.6	.62	.17
52-DC-778B	+40	3.7	.59	.16
52-DC-768A	-40	3.6	.48	.13
52-DC-710A	-40	4.1	.33	.08

this group of samples, no real difference in the amount of thorium is attributable to difference in the size of particles analyzed. Seemingly, the geologic relations and composition of the monazite from the three areas in Georgia can be compared without a bias introduced by hand-picking.

Oconee County. The amounts of thorium in specimens of detrital monazite from Oconee County resemble closely the percentages detected elsewhere in the monazite belt for monazite from rocks of equivalent metamorphic facies. In four analyses (52-PK-177A and B, 52-PK-208A and B) of detrital monazite from distributive provinces underlain by biotitic schist and gneiss of the staurolite-kyanite subfacies grading locally to the sillimanite-almandine subfacies, thoria ranges in percentage from 3.3 to 4.9 and averages 4.2. This is somewhat less thoria than is typically associated with monazite from rocks

of the sillimanite-almandine subfacies in North Carolina, which averages about 4.8 percent ThO_2 (Overstreet, 1967, table 64). The percentage is, however, typical of monazite from schist in the lower subfacies of the amphibolite facies (Overstreet, 1967, p. 18).

In the analyses (52-PK-261A and B) of detrital monazite derived from granite intrusive into schist of the sillimanite-almandine subfacies, the percentage of thoria, 6.0 to 6.1, is identical to the average percentage of thoria (6.1) in monazite from the Toluca Quartz Monzonite in North Carolina where that rock is a synkinematic intrusive into metamorphic rocks of the sillimanite-almandine subfacies (Overstreet, 1967, table 59).

Sillimanite-almandine subfacies rocks and related synkinematic granite are less common in Oconee County than they are in the formerly mined parts of the monazite belt between Morganton, N. C., and Spartanburg, S. C. Consequently, the general tenor in thorium of detrital monazite is less in Oconee County than in the placer district to the northeast.

Spalding County and Pike County. Detrital monazite (52-DC-790A, and 52-DC-791A1-A3, B) derived from biotite granite intrusive into biotite schist and gneiss of probable staurolite-kyanite subfacies has an average of 5.5 percent thoria (Table 2), which is nearly identical to the average percentage of thoria (5.6) in detrital monazite from granitic rocks intrusive into metamorphic rocks of the staurolite-kyanite subfacies in North Carolina (Overstreet, 1967, p. 14).

Harris County and Troup County. The 3.6 average percentage of thoria in detrital monazite from biotite schist and biotite gneiss of staurolite-kyanite subfacies and possibly lower facies in Harris County and Troup County (52-DC-778A and B, and 52-DC-768A) lies between a general average of 3 percent for monazite from metasedimentary rocks of the albite-epidote amphibolite facies and 4.9 percent for monazite from metasedimentary rocks of the amphibolite facies (Overstreet, 1967, p. 18). The monazite from Yellowjacket Creek, Troup County, (52-DC-710A) contains 4.1 percent thoria. The principal source rock is granite intrusive into schist and gneiss of the staurolite-kyanite subfacies. This percentage of thoria is remarkably close to the general average of 4.2 percent ThO_2 found on a worldwide basis for monazite from granite with wallrocks at the lower and middle subfacies of the amphibolite facies (Overstreet, 1967, p. 22), but it is substantially lower than the percentage (5.6) in monazite from granites in wallrocks of staurolite-kyanite subfacies in North Carolina (Overstreet, 1967, p. 14).

Regional aspects. The regional trend in percentage of ThO_2 in detrital monazite from the three areas in Georgia is shown in Table 3. In monazite from Oconee County in the northeast to Harris and Troup Counties in the southwest the thoria progressively decreases. Although in a given locality, absolute abundances of thoria are different between monazite from metasedimentary rocks and monazite from

Table 3. Regional Trend of ThO_2 in Monazite from the Western Monazite Belt in the Carolinas and Georgia, in percent.

	Northeast → Decreasing ThO_2 → Southwest			
Area	North Carolina	Oconee County, Ga.	Spalding County and Pike County, Ga.	Harris County and Troup County, Ga.
General metamorphic grade of schist and gneiss	Sillimanite almandine subfacies widespread a/	Sillimanite-almandine subfacies scarce, staurolite kyanite subfacies common	Staurolite-kyanite subfacies common	Staurolite-kyanite subfacies and lower facies
ThO_2 monazite from schist and gneiss	4.8	4.2	No sample	3.6
ThO_2 in monazite from granitic rocks	6.1	6.0-6.1	5.5	4.1

a/ Overstreet, 1967, table 66.

granites, a parallel decrease in thoria appears to accompany the decrease in regional metamorphic grade. The lack of samples of monazite from schist in Spalding and Pike Counties reduces the strength of the demonstration, but it opens the possibility for an independent test of the thesis. Monazite recovered from metasedimentary rocks in that area might be expected to have between 3.6 and 4.2 percent of ThO_2, possibly around 4.0 percent.

Detrital monazite is far from ideal for an investigation of the trend in abundance of thorium related to genetic aspects of the monazite, because the source rocks of detrital monazite are seldom known with certainty. If rocks are sampled, then an appreciably larger number of samples must be analyzed to arrive at averages for thorium in monazite from a single source rock than is needed when alluvial monazite is used. There is some range in percentage of thoria from samples of individual rocks (Overstreet, 1967, tables 60, 61, 64, 65 and 66), but natural blending in streams tends to narrow this range.

Uranium

Little is known about the geologic relations of uranium in monazite in a general way; thus, few interpretations of the data in Table 2 can be made. With regard to variation by grain size of the monazite, the -40 mesh grains in four (52-PK-208, 52-PK-261, 52-DC-791, and 52-DC-778) of the five samples giving sized fractions from the same source contain from 0.01 to 0.1 percent more U_3O_8 than the +40 mesh grains. In the fifth pair (52-PK-177) the coarser grained monazite has 0.03 percent more U_3O_8.

Some difference is seen between the amount of U_3O_8 in detrital monazite derived mainly from metasedimentary rocks and that from

granite in the same area. Monazite from granite in this region tends to have less U_3O_8 than that from schist:

Area	Average percentage of U_3O_8 in monazite	
	Schist	Granite
Oconee County	0.54	0.44
Spalding County and Pike County	No sample	0.18
Harris County and Troup County	0.58	0.33

No regional variation in the percentage of U_3O_8 could be discerned in these samples of monazite.

Uranium/thorium Ratios

Uranium/thorium ratios of detrital monazite were first discussed in 1953 by Mertie (1953, p. 11-12). From an examination of U_3O_8/ThO_2 in 53 separates of detrital monazite and one sample of monazite from saprolite in North and South Carolina, Mertie postulated that a high content of thorium is not necessarily accompanied by a high content of uranium, that in the area represented by his samples the largest content of U_3O_8 was in monazite with 4.5 to 5 percent ThO_2, and that the observed relationship did not result from any particular geographic distribution or localization. Although the localities of the 53 samples of monazite are given with great care, Mertie was unable to evaluate the probable kinds of source rocks owing to sparsity of detailed geologic maps. Thus, he was unable to show if some geologic control effected the relation he observed.

Mertie's data, summarized in Table 4, show that the mean value of the uranium/thorium ratio is lower for thorium-rich monazite than for thorium-poor monazite (Table 4). The 18 samples of monazite with 6 percent or more ThO_2 have mean uranium/thorium ratios in the range 0.038-0.053 with a weighted average of 0.047, whereas the 36 monazites with less than 6 percent of ThO_2 have uranium/thorium ratios in the range 0.072-0.106 with a weighted average of 0.081.

The interesting possibility exists that there may be a relation between the original rock in which the monazite was formed and the uranium/thorium ratio of the monazite.

In the analyses of detrital monazite from Georgia (Table 2), monazite dominantly from metamorphosed sedimentary rocks has uranium/thorium ratios between 0.11-0.17 and monazite dominantly from granite has uranium/thorium ratios between 0.02-0.08, with respective means of 0.14 and 0.05.

The mean of the uranium/thorium ratios of monazite from granite in Georgia, 0.05, is close to the weighted average ratio of 0.047 for the 18 monazites from North and South Carolina listed by Mertie as having 6 percent or more of ThO_2 (Table 4). Monazite from granitic rocks, pegmatite, and possible orthogneiss in the central part of the

Table 4. Relation of Range in ThO_2 to Mean Value of U_3O_8/ThO_2 in 54 Samples of Monazite From the Carolinas as Described by J. B. Mertie, Jr.
[Modified from Mertie, 1953]

Number of Samples	Range in ThO_2 (percent)	Mean Value of U_3O_8/ThO_2
7	7.84-7.00	0.044
3	6.99-6.50	.038
8	6.49-6.00	.053
10	5.99-5.50	.073
12	5.49-5.00	.072
9	4.99-4.50	.106
5(a)	4.49-2.48	.073

(a) Includes one sample of monazite from saprolite.

area sampled by Mertie has been shown to have averages of 6.0 to 6.9 percent ThO_2, whereas monazite from the paraschists contains an average of 4.8 percent ThO_2 (Overstreet, 1967, Tables 64-66). The low uranium/thorium ratios found for detrital monazite from granitic sources in Georgia correspond to low ratios found by Mertie for detrital monazite with more than 6 percent ThO_2 in the Carolinas. The possibility exists that the monazite with more than 6 percent ThO_2 may have been largely derived from granitic sources in the Carolinas, and the division of monazite by percentage of ThO_2 given by Mertie is in part a natural division related to the origin of the monazite.

Detrital monazite derived mainly from metamorphosed sedimentary rocks (schist) in Georgia has a mean uranium/thorium ratio of 0.14, and this monazite contains 3.3-4.9 percent ThO_2. The weighted average of the mean uranium/thorium ratios cited by Mertie for 14 monazites with 2.48 to 4.99 percent ThO_2 is 0.094 (Table 4). These monazites approach but do not equal in uranium/thorium ratios the Georgia monazites derived mainly from schist. The difference between the uranium/thorium ratios is appreciably narrowed, however, if the comparison is taken between the uranium/thorium ratios of the highest grade source rocks in Georgia, those from Oconee County, where the ratio for the monazite is 0.12. For the lower-grade source rocks in Harris and Troup Counties, the uranium/thorium ratio increases to an average of 0.15.

These regional relations suggest the possibility that average uranium/thorium ratios on the order of 0.05 may be associated with monazite derived from granite with wallrocks at the sillimanite-almandine subfacies if the monazite also contains about 6 percent of ThO_2. Monazite with mean uranium/thorium ratios around 0.09 and an average

of 4.8 percent ThO_2 may be mainly derived from sedimentary rocks at the sillimanite-almandine subfacies of regional metamorphism. Monazite with uranium/thorium ratios around 0.12-0.15 and average ThO_2 around 3.6 to 4.2 percent may come mainly from sedimentary rocks at the staurolite-kyanite or lower subfacies. Monazite with uranium/thorium ratio around 0.08 and ThO_2 around 4 percent may come from granite intrusive into metamorphic rocks of dominently lower grade than the staurolite-kyanite subfacies.

These suggested interpretations are tentative. More precise data, based on many analyses of monazite from crystalline rocks, are needed to prove the relationship is real. Georgia and the Carolinas offer a convenient place to test the interpretation, because monazite can be collected readily from crystalline rocks by panning saprolite or by crushing and panning the unweathered rock. The validity of uranium determinations on either detrital monazite or the monazite in saprolite should be determined by comparing the results with analyses of monazite from unweathered samples of the same source rock.

POSSIBLE ECONOMIC SIGNIFICANCE OF THE COMPOSITION OF GEORGIA MONAZITES

Possibly one of the reasons monazite was not mined in Georgia during the lifetime of the industry in the Carolinas was that the average tenor in thorium of the Georgia monazite was too low. If the monazite was too lean in thorium to meet market specifications of the times, then it seems likely that commercial analyses would have been made to establish this fact, but none is known in the literature except the one by Pratt (1916, p. 40) reporting 4 percent ThO_2 in monazite from a gold placer in northern Georgia. This amount is lower than the 5 to 6 percent of thoria mentioned by Kremers (1958, p. 2) for Carolina commercial concentrates. It is also somewhat lower than the average of 4.8 percent thoria reported here for placer monazite from the Georgia Piedmont, and the 4.42 percent of ThO_2 reported by Mertie (1953, p. 12) for one sample from Spalding County.

Locally, as in the granitic areas in Oconee, Spalding, and Pike Counties, detrital monazite is known that has 5 to 6 percent of thoria (Table 2) and matches in tenor the range reported by Kremers for Carolina commercial concentrates. However, no monazite containing 6.5 percent or more thoria, like that found by Mertie for nearly 20 percent of the samples he took in formerly-mined streams in the Carolinas (Table 4), is known in Georgia. Commercial concentrates tend to be somewhat leaner in ThO_2 than the handpicked monazite reported here, owing to admixture of other minerals; thus, most monazite concentrates from stream placers in the Piedmont of Georgia probably would contain less than 5 percent of ThO_2.

SUMMARY

The decrease in percentage of thorium in monazite southwestward from the center of monazite mining in the Carolinas is paralleled by a decrease in regional metamorphic grade of gneiss and schist that underlie the monazite-bearing streams and are partly the source of the monazite. At the border between North and South Carolina the placers are found over schist and gneiss of the sillimanite-almandine subfacies and over syntectonic quartz monzonite (Overstreet and Bell, 1965, pl. 3). In the Oconee County area rocks of sillimanite-almandine subfacies are present but they are scarce; the dominant rocks are at the staurolite-kyanite subfacies. Farther southwestward in Georgia along the monazite belt the sillimanitic rocks tend to disappear, and rocks of the staurolite-kyanite subfacies and of lower metamorphic facies are present. It has previously been shown that the amount of thorium in monazite is related to the metamorphic facies of the source rock: monazite in rocks of the highest metamorphic facies contains the most thorium (Overstreet, 1960, p. B56). The tenors in thorium of the Georgia monazites here reported are appropriate for the regional metamorphic facies of the rocks underlying the basins from which the detrital monazite came.

Uranium/thorium ratios in the monazite may be controlled by the mode of origin of monazite in such a way that low ratios associated with high thorium indicate a granitic source, and high ratios associated with low thorium indicate sources in paragneiss or paraschist. Further test of this thesis is needed.

Monazite with commercially acceptable tenors in thorium is present locally in Georgia, but it is more restricted in areal extent than it is in the Carolinas where alluvial placers were formerly mined for monazite.

REFERENCES CITED

Engineering and Mining Journal, 1888, Extended use of some of the rarer minerals: Eng. Mining Jour., v. 46, no. 1, p. 1 and 2.

Fletcher, M. H., Grimaldi, F. S., and Jenkins, L. B., 1957, Thoron-meso-tartaric acid system for the determination of thorium: Anal. Chemistry, v. 29, p. 963.

Grimaldi, F. S., May, Irving, Fletcher, M. H., and Titcomb, Jane, 1954, Collected papers on methods of analysis for uranium and thorium: U. S. Geol. Survey Bull. 1006, 184 p.

Hewett, D. F., and Crickmay, G. W., 1937, The warm springs of Georgia, their geologic relations and origin--a summary report: U. S. Geol. Survey Water-Supply Paper 819, 40 p.

Kremers, H. E., 1958, Commercial thorium ores: Soc. Mining Engineers of Am. Inst. Mining Metall. Engineers, preprint 5819A18, p. 1-14.

May, Irving, and Jenkins, L. B., 1965, Use of arsenazo III in determination of thorium in rocks and minerals: U. S. Geol. Survey Prof. Paper 525-D, p. D192-D195.

Mertie, J. B., Jr., 1953, Monazite deposits of the southeastern Atlantic states: U. S. Geol. Survey Circ. 237, 31 p.

_____, 1955, Ancient monazite placer (abs.): Geol. Soc. America Bull., v. 66, no. 12, pt. 2, p. 1692-1693.

_____, 1956, Paragneissic formations of northern Virginia (abs.): Geol. Soc. America Bull., v. 67, no. 12, pt. 2, p. 1754-1755.

_____, 1957, Geologic occurrence of monazite and xenotime in the southeastern states (abs.): Geol. Soc. America Bull., v. 68, no. 12, pt. 2, p. 1766-1767.

Murata, K. J., and Bastron, Harry, 1956, A convenient method for recognizing nonopaque cerium earth minerals: Science, v. 123, no. 3203, p. 888-889.

Overstreet, W. C., 1960, Metamorphic grade and abundance of ThO_2 in monazite: U. S. Geol. Survey Prof. Paper 400-B, p. B55-B57.

_____, 1967, The geologic occurrence of monazite: U. S. Geol. Survey Prof. Paper 530, 327 p.

Overstreet, W. C., and Bell, Henry, III, 1965, The crystalline rocks of South Carolina: U. S. Geol. Survey Bull. 1183, 126 p.

Overstreet, W. C., Theobald, P. K., Jr., and Whitlow, J. W., 1959, Thorium and uranium resources in monazite placers of the western Piedmont, North and South Carolina: Mining Eng., v. 11, no. 7, p. 709-714.

Overstreet, W C., Yates, R. G., and Griffitts, W. R., 1963, Heavy minerals in the saprolite of the crystalline rocks in the Shelby quadrangle, North Carolina: U. S. Geol. Survey Bull. 1162-F, 31 p.

Parizek, E. J., 1953, A preliminary investigation of the geology of Clarke County, Georgia: Georgia Geol. Survey Bull. 60, pt. 2, p. 21-31.

_____, 1955, Xenoliths in granodiorites of the east Georgia Piedmont: Georgia Acad. Sci. Bull., v. 13, no. 3, p. 85-89.

Pratt, J. H., 1916, Zircon, monazite, and other minerals used in the production of chemical compounds employed in the manufacture of lighting apparatus: North Carolina Geol. Survey Bull. 25, 120 p.

Stose, G. W., and Smith, R. W., 1939, Geologic map of Georgia: Georgia Div. Mines, Mining and Geology, scale 1:500,000.

X-RAY ANALYSES OF ROCKS OF THE CAROLINA SLATE BELT, UNION COUNTY, NORTH CAROLINA

By

Anthony F. Randazzo
Department of Geology
University of North Carolina
Chapel Hill, North Carolina 27514*

ABSTRACT

Fifty-seven samples were collected from a variety of low-rank metamorphic rocks in Union County, North Carolina. Modal analyses of these samples were performed by means of X-ray diffraction techniques. Semi-quantitative results were obtained. These data, however, provide at least some measure of the mineral percentages in the extremely fine-grained meta-volcanic and epiclastic rocks. Composition of the argillites and sandstones are very similar despite stratigraphic position. These data also show a relatively high proportion of quartz in many samples suggesting an episode of silicification which probably accompanied metamorphism.

INTRODUCTION

The Union County portion of the Carolina Slate Belt is particularly interesting because the rocks there have retained sedimentary characteristics even though subjected to low rank metamorphism. A detailed lithologic and stratigraphic study was undertaken in order to reconstruct the geologic history of the region (Randazzo, 1968). One of the major problems encountered was the determination of mineral percentages in the various rock types. Another was the correlation of stratigraphic units by recognizable mineral zones. Many of the rocks in the Union County area are extremely fine grained, frustrating attempts to study them microscopically. X-ray diffraction methods were utilized to determine modal compositions.

Acknowledgments

The writer extends thanks to Paul C. Ragland and Daniel A. Textoris for their valuable suggestions and assistance in the investigative and writing stages of the project. Financial support was

*Present Address: Department of Geology, University of Florida, Gainesville, Florida 32601

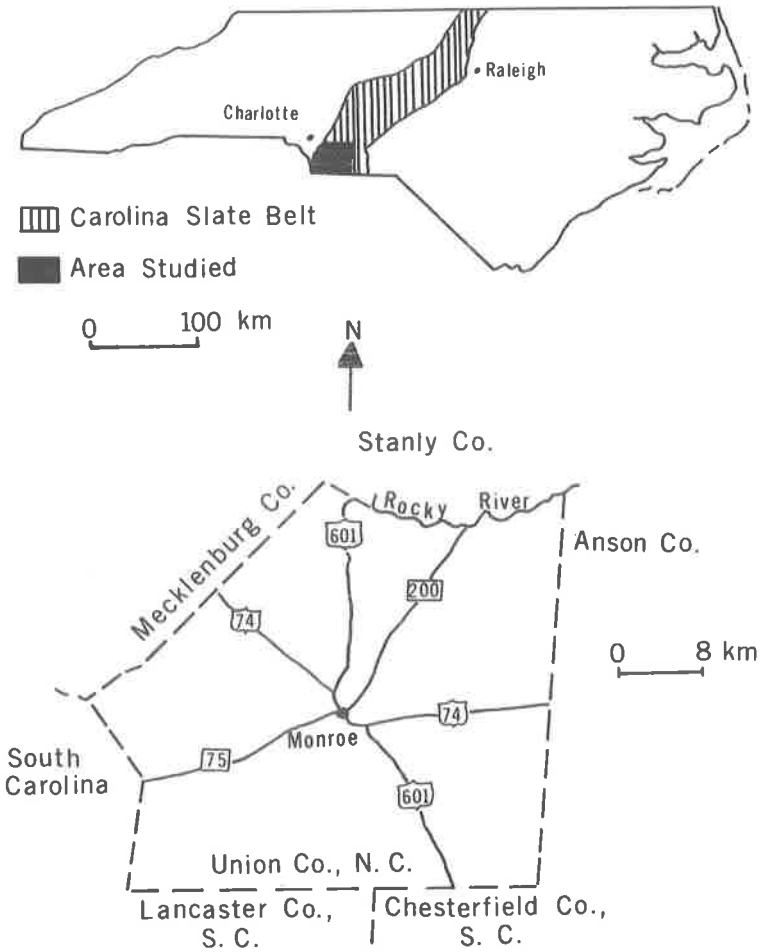

Figure 1. Index map of the Carolina Slate Belt in North Carolina and Union County.

provided by a National Science Foundation Student Research Fellowship, The Society of the Sigma XI, Division of Mineral Resources of the North Carolina Department of Conservation and Development, and the Smith Fund of the University of North Carolina.

GEOLOGIC SETTING

The Carolina Slate Belt extends across Virginia, North Carolina, South Carolina and Georgia in a northeast-southwest direction. This belt of low rank metamorphic volcanic and sedimentary rocks is situated in the east-central portion of the Piedmont of North Carolina (Figure 1). Coastal Plain sediments overlap the Slate Belt from the

east while the Charlotte Belt, consisting of higher rank metamorphic and igneous rocks, borders it on the west. The Deep River and Wadesboro Triassic Basins surficially bifurcate the Slate Belt in North Carolina where its outcrop width is greatest. In Union County, the Carolina Slate Belt is bordered on the east by the Wadesboro Triassic Basin and on the west by the Charlotte Belt.

Four formations are recognized in the Union County portion of the Carolina Slate Belt. Stratigraphic names are from Conley and Bain (1965). The Uwharrie Formation represents a period of extensive volcanism with the formation of crystal lithic and devitrified tuffs. The Tillery Formation consists of thin bedded, laminated argillite with some interbedded nonlaminated argillite and sandstone. Thick bedded, tuffaceous argillite characterizes the McManus Formation which also contains an appreciable amount of crystal tuff and very fine-grained sandstone. The youngest unit is the Yadkin Graywacke which consists of thick bedded graywacke and laminated argillite. Quartz and igneous intrusions are found in all of the units. Age of the Slate Belt rocks is still speculative. Documented fossils (St. Jean, 1965, p. 307) and radiometric age determinations (White and others, 1963; Hills and Butler, 1968) indicate Cambrian and Ordovician.

PROCEDURE

The analytical procedure used was modified after Tatlock (1966) and Butler and Ragland (1968) and is based on the principal that relative intensities of X-ray patterns are directly proportional to the concentrations of the minerals present. In order to make this method applicable, reproducibility is cardinal. Reporducibility is possible only when complete random orientation or perfect alignment of particles is achieved. Random orientation is more practical and can be most nearly attained by using very finely ground powders (Tatlock, 1966, p. 5).

Representative samples were chipped from 57 selected whole rock specimens, crushed by hand, and ground in a power mortar and pestle for 20 minutes. This interval of time was usually sufficient to allow the sample to pass through a 325 mesh sieve (particle size less than 44μ). Crushing and grinding were sometimes completed in increments so that the whole sample would be represented. Thorough mixing of the samples was assured by using the Spex Corporation Mixer-Mill device.

The powdered samples were mounted in standard aluminum sample holders. The mounting process consisted of pouring the sample into a holder which rested on a sheet of semi-glossed paper. The sample was firmly compressed into the holder and excess powder was scraped away leaving a smooth packed surface. The holder could then be picked up gently, being particularly careful not to slide the holder over the paper. The side which was in contact with the paper was

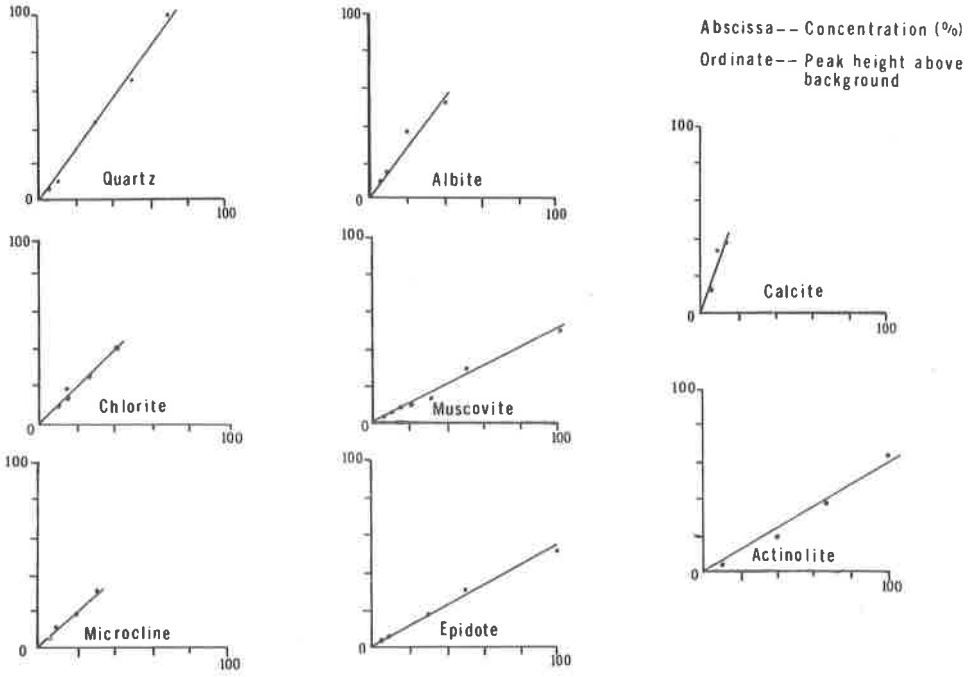

Figure 2. Calibration curves for the mineral standards used in X-ray analyses.

exposed to X-rays. This mounting procedure insured a reasonable degree of random orientation for the powder.

A Philips X-ray diffraction unit was calibrated by using standard rock powders supplied by J. Robert Butler and Paul C. Ragland. These standards were prepared by mixing measured weight percentages of quartz, microcline, albite, muscovite, actinolite, epidote, chlorite and calcite. Calibration curves for these minerals are presented in Figure 2. Calibration of the diffraction unit was checked periodically with a standard mount to determine instrument drift. Actual instrumentation settings used may be summarized as follows:

Copper Tube: 35 Kv; 18 Ma; Nickel Filter; Scintillation Counter
Goniometer Scanning Speed: 1°/min; Recorder Chart Speed: 1/2 in./min.
Goniometer Slits: Diverging 1°; Scatter 1°; Receiving 0.006"
Ratemeter: Scale Factor 10^2 or 10^3; Multiplier 1 or 2; Linear Scale
Time Constant: 2 Detector Voltage: 0.98 Kv
Pulse Height Analyser: Level 4; Window 16

The peaks selected from the X-ray patterns for measurement were based on the degree of intensity and the number of minerals having a peak at a particular 2θ position. Generally, those peaks chosen

Table 1. X-Ray Diffraction Peaks Used for Calculating Mineral Percentages

Mineral	2θ	d-spacing	hkl
Muscovite	8.9°	10.0 A	002
Actinolite	10.5°	8.42 A	110
Chlorite	12.5°	7.08 A	002
Quartz	20.8°	4.26 A	100
Microcline	27.5°	3.24 A	$2\bar{2}0$, 002, 040
Albite	27.9°	3.19 A	002
Calcite	29.5°	3.02 A	104
Epidote	30.9°	2.89 A	$11\bar{3}$

had relatively high intensities but were not significantly superposed by peaks of the other common minerals (Table 1). The peak used for microcline (27.5°2θ) was scanned at a slower speed (1/4°2θ/min.) in an attempt to avoid interference by other mineral reflections. Duplicate runs were made on all samples and where significant differences occurred, a third run was made. Measured peak heights were compared with the established calibration curve for each mineral. Total mineral percentages for each sample ranged from 80 to 140 percent. Generally, felsic samples yielded total mineral percentages greater than 100 while mafic sample values were less than 100. They were adjusted to a total of 100 percent in an attempt to correct for differences in the mass-adsorption coefficients of the various constituents. This correction is a more convenient method of utilizing relative peak heights, thus avoiding many of the problems associated with absolute intensities.

RESULTS

The results obtained were semi-quantitative because of the fluctuations of peak heights in some of the unknowns. Precision for the duplicate runs made on the samples ranged from less than 1 to more than 5 weight percent. Peak height fluctuations were attributed to: (1) compositional variations within individual minerals; (2) electronic instability of the instruments; (3) failure to achieve complete random

orientation of particles; (4) insufficient correction of data for the different mass-adsorption coefficients of the minerals; and (5) presence of minerals for which no standard was available. Two such substances were kaolinite and 14 Å chlorite-like intergrade material that have intense peaks coincident with those used for chlorite percentage determinerations (7.00 Å line). The 7.00 Å line, therefore, represents the combined percentage of chlorite, kaolinite and 14 Å chlorite-like intergrade material in the rock, and this combination was reported as such. Because the chlorite calibration curve was used, an unavoidable error was introduced. The same situation exists when biotite was present. In the area studied, this mineral was rarely recognized in thin section. It has, however, an intense peak coincident with that used for the determination of muscovite percentages (10.0 Å line). Biotite can be distinguished from muscovite by the 1.53-1.54 Å line but in quartz-rich rocks this line is masked by quartz (211). The 10.0 Å line, therefore, represents a combined percentage if both minerals are present. Thus, reported chlorite and muscovite percentages are the least confident.

Modal analyses with a microscope were conducted in five of the coarsest-grained specimens in order to check the accuracy of the X-ray technique. Grain size, however, still dictated lumping together of fine-grained material. Results obtained from these two different methods were somewhat similar (Table 2). The X-ray technique, although semi-quantitative, provided at least some measure of the actual percentages of each mineral present in a very fine-grained rock.

Mineral percentages calculated from this X-ray technique were categorized according to formation and rock type. Modal composition for each of these rock types was computed (Table 3). In addition, triangular compositional diagrams were constructed for the argillites and sandstones (Figure 3). Except for the amount of finely disseminated biotite which could not be ascertained, mineral assemblages of each rock type were similar to those found by Butler and Ragland (1968). The characteristic felsic tuff assemblage was quartz-albite-muscovite-chlorite $\pm$ epidote $\pm$ microcline. Mafic tuffs consisted of chlorite-actinolite-albite-epidote $\pm$ quartz $\pm$ muscovite. Argillites (laminated and tuffaceous) and assorted sandstone contained quartz-albite-muscovite-chlorite $\pm$ epidote $\pm$ microcline $\pm$ actinolite. Impure chert mineral assemblage was quartz-albite $\pm$ muscovite $\pm$ chlorite.

GEOLOGICAL IMPLICATIONS

Sedimentation

The triangular compositional diagrams constructed for the argillites and sandstones of the Tillery, McManus and Yadkin units (Figure 3) display a consistency in mineral composition. Petrographic analyses of the Union County rocks (Randazzo, 1968) revealed the

Table 2. Comparison of Modal Composition of Coarser-Grained Rocks Based on Point Counting with a Polarizing Microscope and X-Ray Analyses*

Mineral	McManus Formation Felsic Crystal Tuff #10 pts. counted	%	X-Ray %	McManus Formation Felsic Crystal Tuff #15 pts. counted	%	X-Ray%	McManus Formation Felsic Crystal Tuff #20 pts. counted	%	X-Ray %
Quartz	282	34.0	37	219	21.4	25	204	20.8	20
Muscovite	157	18.9	12	176	17.2	17	143	14.8	14
Chlorite	21	2.5	trace	125	12.2	9	109	11.3	4
Albite	369	44.5	51	502	49.1	49	518	53.1	62

Mineral	McManus Formation Siliceous Siltstone #284 pts. counted	%	X-Ray %	Tillery Formation Argillite #139 pts. counted	%	X-Ray %
Quartz	670	54.6	45	279	30.1	24
Muscovite	248	20.2	24	202	21.8	25
Chlorite	275	22.4	27	158	17.0	15
Albite	36	2.9	5	161	17.3	20
Epidote				128	13.8	16

* Percentages derived from point counting are relative based on the deletion of amorphous and opaque material and the equal distribution of unidentifiable low birefringent material to chlorite, muscovite, albite, and epidote.

Table 3. Average Modal Composition of Each Rock Type Based on X-Ray Analyses (given in percent).

Mineral	Uwharrie Fm.	Tillery Fm.				McManus Fm.			Yadkin Gywke.
	felsic crystal tuff	argillite	felsic intermediate crystal tuff		mafic crystal tuff	impure chert	argillite	felsic crystal tuff	impure chert	sandstone and argillite
quartz	28	26	40	12	2	32	29	32	49	21
muscovite	13	38	3	13	7	29	35	15	11	30
chlorite	4	16	1	32	13	26	15	4	2	31
albite	26	16	56	18	26	14	19	49	38	18
epidote	10	3		25	9	1				
actinolite					45	trace				
calcite	2									
microcline	16									
total	99	99	100	100	102	102	98	100	100	100

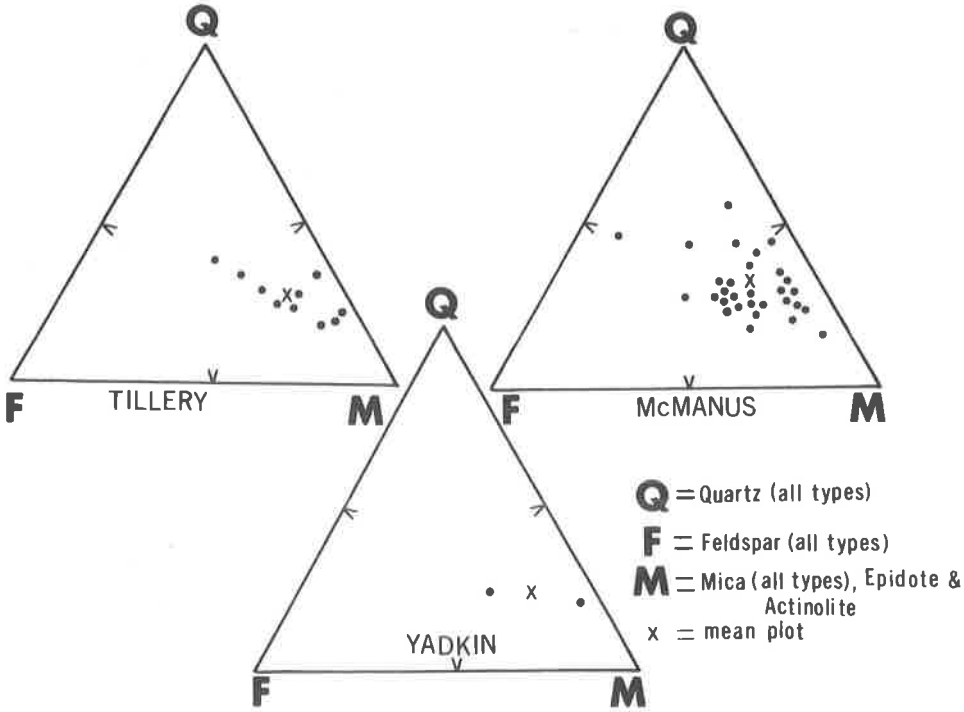

Figure 3. Compositional diagram of sandstones and argillites of the Tillery, McManus and Yadkin units based on X-ray analyses.

occurrence of several different episodes of pyroclastic and epiclastic deposition. The data obtained from X-ray analyses indicate no change in the composition of the source material during these phases of sedimentation. Rocks comprising the formations present must have been almost completely derived from the great amount of volcanic material produced.

Silicification

Another aspect of these semi-quantitative results is the relatively high proportion of quartz in certain argillite samples. Abundance of quartz can be attributed to a post-depositional stage of silicification in the rocks of this region. Field and petrographic studies have shown that quartz veins, quartz cavity fillings and quartz overgrowths are a common occurrence and are closely associated with the more siliceous argillites. Data presented by Butler and Ragland (1968) in the form of triangular plots of major minerals also show evidence of silica mobility, probably accompanying metamorphism.

Metamorphism

X-ray modal analyses indicate that the most abundant minerals present in the rocks of Union County are quartz, albite, muscovite, chlorite and epidote. This assemblage is typical of the quartz-albite-muscovite-chlorite subfacies of the greenschist facies. Pressure and temperature ranges characteristic of this subfacies are 3,000 to 8,000 bars and 300° to 500° C (Turner and Verhoogen, 1960, p. 534). These low pressure and temperature conditions resulted in the low rank regional metamorphism distinctive of this portion of the Carolina Slate Belt.

Rocks in the Albemarle area, North Carolina, are reported to be in the quartz-albite-muscovite-biotite-chlorite subfacies of the Abukuma-type greenschist facies (Butler and Ragland, 1968). The inability to accurately determine percentages or occurrences of biotite in the Union County rocks does not justifiably allow the assignment of this subfacies of the Abukuma-type facies series to the region studied.

SIGNIFICANCE OF THIS TECHNIQUE

The specific aim of the X-ray technique used, as stated by Tatlock (1966, p. 2), is to "permit reasonably accurate and rapid estimates of many common felsic minerals." The use of petrographic methods in modal analyses of extremely fine-grained rocks is not applicable. X-ray diffraction methods provide the only means of finding mineral percentages. The procedure outlined here, although semi-quantitative, provides some insight as to mineral percentages of fine-grained rocks. Without it, no modal information would be known.

REFERENCES CITED

Butler, J. R., and Ragland, P. C., 1968, Low-rank metamorphism of igneous rocks in the Albemarle area, North Carolina Slate Belt: submitted for publication.

Conley, J. F., and Bain, G. L., 1965, Geology of the Carolina Slate Belt west of the Deep-River-Wadesboro Triassic Basin, North Carolina: Southeastern Geology, v. 6, p. 117-138.

Hills, F. A., and Butler, J. R., 1968, Rubidium-strontium dates for some rhyolites from the Carolina Slate Belt of the North Carolina Piedmont (abstract): Prog. Geol. Soc. America, 1968, Southeastern Sec. Mtg., Durham, p. 45.

Randazzo, A. F., 1968, Petrography and stratigraphy of the Carolina Slate Belt, Union County, North Carolina: Unpub. Ph. D. Dissert., Univ. North Carolina, Chapel Hill, 79 p.

St. Jean, J. Jr., 1965, New Cambrian Trilobite from the Piedmont of North Carolina (abstract): Geol. Soc. America Sp. Paper 82,

Tatlock, D. B., 1966, Rapid modal analyses of some felsic rocks from calibrated X-ray diffraction patterns: U. S. Geol. Survey, Bull. 1209, 41 p.

Turner, F. J., and Verhoogen, J., 1960, Igneous and Metamorphic Petrology: New York; McGraw-Hill Book Co., 2nd ed., 694 p.

White, A. M., Stromquist, A. A., Stern, T. W., and Westley, H., 1963, Ordovician age for some rocks of the Carolina Slate Belt in North Carolina: U. S. Geol. Survey Prof. Paper 475-C, p. 107-109.

TOPOGRAPHY OF THE CONTINENTAL MARGIN OFF THE CAROLINAS

By

John G. Newton
and
Orrin H. Pilkey
Duke University Marine Laboratory
and Geology Department

ABSTRACT

A topographic chart of the continental margin off the Carolinas has been prepared with a contour interval of 100 meters. The data are also presented in the form of a block diagram. The sounding data were acquired by Duke University's R/V EASTWARD during cruises between October 1964 and August 1968. The major features of the continental margin in this area include a well developed continental slope - continental rise system and the northern tip of the Blake Plateau. The Hatteras Outer Ridge is found at the base of the rise. Crossing the slope and rise and ending at the Hatteras abyssal Plain is the Hatteras canyon system which is dendritic in form with 3 main tributaries.

INTRODUCTION

Detailed knowledge of the bathymetry of the continental margin is an essential prerequisite for exploring and understanding the nature of sea floor processes. It has, for example, been well established that topography plays a significant role in sedimentation. The need for more bathymetric data in the specific study area of this report was pointed out by Gorsline (1963).

The establishment of the Duke University Cooperative Oceanographic program in 1962 resulted in an intensification of continental margin oceanographic studies off North Carolina. The EASTWARD program in itself created a need for detailed topographic coverage of the area. Until recently the only available information has been the individual soundings published on various U. S. Coast and Geodetic Survey and U. S. Naval Oceanographic Office charts. During more than 4 years of operation of the Duke University research vessel EASTWARD, from its home port of Beaufort, North Carolina, precision depth records have been accumulated over several thousand miles of ship tracks. These records are stored in the Oceanographic program files at the Duke University Marine Laboratory, in Beaufort, North Carolina,

and are available for study by any qualified marine investigator. The EASTWARD soundings form the principal basis for construction of both the bathymetric chart (Plate I) and block diagram (Plate II).

Heezen, Tharp, and Ewing's (1959) physiographic diagram of the North Atlantic Ocean Basin is useful but it is a generalized and small-scale characterization of the sea floor. Uchupi (1966) published a series of topographic charts of the Eastern U. S. Continental Margin with 200-meter contour intervals at a scale of 1:1,000,000. Rona, Schneider and Heezen (1967) have presented the most recent and detailed bathymetric chart. In addition to showing the general nature of the Carolina Continental Rise, they recognized three branches of the complex Hatteras Canyon System. They also described the morphology of the Hatteras Outer Ridge at the base of the continental rise.

In this discussion of bathymetry, the classification and definitions of sea floor physiographic features presented by Heezen, Tharp, and Ewing (1959) are used. The three second order physiographic features of the ocean basin are, according to these workers, the continental margin, the ocean basin floor and the mid-ocean ridge. This report is concerned with the continental margin off North and South Carolina. Features within this second order province include the continental shelf, the continental slope, the continental rise as well as a portion of a marginal plateau (the Blake Plateau).

Acknowledgements

Precision depth profiles used to compile these figures were obtained from the files of the Cooperative Program in Biological Oceanography at the Duke University Marine Laboratory under the direction of C. G. Bookhout. The authors are indebted to the many investigators who acquired these profiles during their cruises and to those who have granted permission for the use of profiles in the construction of Plates I and II. R/V EASTWARD officers, commanded by Captains Milan Willis, William Craig and David Beveridge provided the adjusted navigation tracks critically needed for the construction of the sounding collection charts. The Oceanographic Party Chiefs George Newton, Thomas Pinner, James Cason and Thomas Dow have diligently attended the depth recorders and instructed scientific participants to assure good profiles. Mr. David Murphy, chief mate, provided many of the base charts used for navigation and adjusted the ship's tracks to assure accuracy.

Much of the credit for Plates I and II is due to the untiring efforts of Miss Rita Duncan and Miss Linda Burrows who did the painstaking data compilation and the transposition of the contour chart to the block diagram. Many others, including investigators and potential users, offered beneficial suggestions concerning the contour chart and block diagram.

Operation of the R/V EASTWARD through which these data

were collected is supported by the National Science Foundation on grant number GB-0869. The scientific research and training program has complementary funding on grant number GB-8189. Data processing, initial plotting and diagram construction were accomplished through funding by the North Carolina Board of Science and Technology. Various aspects of data processing during the latter part of this investigation were supported by the U. S. Geological Survey.

METHODS

Construction of the bathymetric chart followed the standard method of reading individual depths from the precision echo sounding records, plotting these at five minute intervals on each adjusted cruise track and later compiling the depths from many tracks on a sounding collection chart. After examining the validity of individual soundings the collection sheet was contoured. Frequent reference was made to individual profiles for assistance in contouring.

Construction of the block diagram was acheived by a four stage projection directly from the contour chart as described by Stacey (1958). This simple step by step process yields a three-dimensional representation combining the advantage of perspective with that of accurate location of features.

DISCUSSION

The Continental Shelf

In the map area, the continental shelf break lies entirely shoaler than 100 meters and is typically found between 40 and 80 meters. In some locations, depth of the shelf break may be controlled by the existence of a trough and reef-like structure extending intermittently along the shelf edge between Cape Hatteras and Cape Fear, North Carolina. (Menzies et al., 1966; Macintyre and Milliman, in press). The continental shelf ranges in width from less than 16 miles off Cape Hatteras to over 60 miles in the center of Long Bay (between Cape Fear and Cape Romain). The shelf has an average slope of less than 1:900. The most prominent topographic features on the shelf are the NW-SE trending shoals associated with each of the capes. Rock outcrops are common on the shelf, particularly in Onslow Bay (between Cape Lookout and Cape Fear), because of the relatively low rates of present-day sedimentation (Cleary and Pilkey, 1968). No well-defined or consistent wave-built or wave-cut terrace like features related to previous shorelines were observed.

The Continental Slope

The continental slope, by definition, exhibits a greater declivity than either the continental shelf or the continental rise and occurs between these two features. The distinction between the continental slope and the continental rise is particularly evident in this area, as illustrated in both Plates I and II. The base of the continental slope occurs at a depth of approximately 1600 meters north of Cape Hatteras and becomes progressively deeper to the southeast of Cape Lookout where the slope extends to 2,700 meters. The width of the continental slope ranges from 7 to 8 miles in the vicinity of Cape Hatteras to over 25 miles southeast of Cape Lookout. The continental slope exhibits a gradient of about 1:10 off Cape Hatteras, which is the area of maximum declivity. The gradual broadening of the continental slope south of Cape Hatteras represents the northernmost extremity of the Blake Marginal Plateau, called the Blake Plateau Nose. Details of the topography of the Blake Plateau have been discussed by Pratt and Heezen (1962).

Striking topographic irregularities of various kinds exist on the slope off Cape Hatteras that cannot be clearly defined with the presently available sounding data. The origin of these features is an interesting problem that bears on the fundamental question of the origin of continental slopes. Obviously, some of these irregularities are canyon tributaries; others may be slump structures or resistant ledges of outcropping rocks.

The Continental Rise

The continental rise is about 150 miles in width in the area of investigation. The average slope is approximately 1:100, but the slope is less on the lower rise compared to that of the upper rise. The base of the continental rise is found in depths close to 5,200 meters where it merges with the Hatteras Abyssal Plain.

A number of topographic features are present on the surface of the continental rise, the most prominent of which is the Hatteras Canyon System. To the north and northeast is found the single, relatively straight channel of the Norfolk Canyon. Along the southern margin of the mapped area, east of the Blake Plateau Nose, is a very broad valley essentially beginning on the upper rise and ending on the lower rise. The broad Hatteras Outer Ridge, at the base of the continental rise, trends NE-SW and exhibits a maximum local relief of about 400 meters. The northeasterly extent of this ridge-form is unknown (Rona et al., 1967). Minor topographic features on the continental rise include the ill-defined "humps", particularly in the vicinity of the Hatteras Canyon System. These are probably slump structures.

The complex Hatteras Canyon System occurs in an area 70 miles in width trending NW-SE off Cape Hatteras. Rona, et al., (1967)

recognized three principle tributaries two of which they called the Pamlico (most southerly branch) and Hatteras canyons respectively. At the base of the rise, trending parallel to, and landward from, the Hatteras Outer Ridge they recognized the Transverse Canyon. The more detailed bathymetric data available for this study reveals that the canyon system differs in two important respects from previous interpretation. First, the Hatteras Canyon system appears to form a complicated dendritic pattern of major and minor tributaries, rather than a simpler pattern of relatively straight channels with few, if any, tributaries. Secondly, the Transverse Canyon appears to continue up the rise onto the lower continental slope instead of ending on the lower continental rise, as previously believed. We propose that this branch of the canyon be recognized as a distinct unit of the canyon system and that it be called the "Albemarle Transverse Canyon."

Only one branch (Hatteras Canyon branch) has tributaries that extend up to and actually indent the shelf edge. The canyon tributaries tend to be broad with relatively gentle sides on the lower rise; on the upper rise and on the slope, however, the canyons are narrow and steep walled. Canyon relief is usually between 100 and 200 meters. A clearly developed system of natural levees is present on the southwest side of the major tributaries, or on the right side of flow direction, but are seldom present on the northeast (left side of flow direction) side. The levees exhibit a maximum local relief of 50 meters, but more typically are about 30 meters high.

The classical explanation for better developed natural levee systems on the "right" side of submarine canyons is the effect of Coriolis Force on moving bodies in this hemisphere (Shepard and Dill, 1966). On the Carolina shelf deep bottom currents almost exclusively flow from northeast to southwest (Heezen, Hollister and Ruddiman, 1966) and these quite likely play a role in increasing the rate of sedimentation on the southwest side of the canyon tributaries.

There are several explanations for the occurrence of the Hatteras Canyon system off Cape Hatteras. The most important is probably the fact that in this area the Gulf Stream turns away from the continental margin and begins its flow over deeper waters. This, in addition to the termination of the relatively shallow Blake Plateau where the canyon begins, means that Gulf Stream's suspended material will begin to be deposited and will form an important source of material for turbidity current flows. Another important factor in the location of the canyon is that fine Recent sediments are being carried out beyond the shelf break off Cape Hatteras in a wide band paralleling both sides of Diamond Shoals. Shoals perpendicular to the other Carolina Capes also cause transportation of material to the upper continental slope but here the Gulf Stream prevents significant accumulation. Probably the sediment transported out along the Hatteras shoal system acts as a point source of sediment. However, the Gulf stream should not act as a point source. Thus, the explanation for the 70 mile width and, probably,

also for the dendritic pattern may be related to the broad area of deposition of Gulf Stream material.

REFERENCES CITED

Cleary, W. J., and Pilkey, O. H., 1968, Sedimentation in Onslow Bay: Southeastern Geology, Spec. Publ. 1, 1-17.

Heezen, Bruce C., Tharp, Marie, and Ewing, M., 1959, The floors of the oceans - I. The North Atlantic: Geol. Soc. America Spec. Pap. 65, 122 p.

Heezen, B. C., Hollister, C. D., and Ruddiman, W. F., 1966, Shaping of the Continental Rise by deep geostrophic contour currents: Science, v. 152, p. 502-508.

Gorsline, D. S., 1963, Bottom sediments of the Atlantic Shelf and Slope off the Southern United States: Jour. Geol., v. 71, p. 422-440.

Macintyre, I. G., and Milliman, J. D., in preparation, Physiographic features on the outer shelf and upper slope, continental margin, SE U. S.

Menzies, R. J., Pilkey, O. H., Blackwelder, B. W., Dexter, D., Huling, P., and McCloskey, L., 1966, A submerged reef off North Carolina: Int. Revue ges. Hydrobiol., v. 51, p. 393-431.

Pratt, R. N., and Heezen, B. C., 1962, Topography of the Blake Plateau, Deep Sea Res., v. 11, p. 721-728.

Rona, P. A., Schneider, E. D., and Heezen, B. C., 1967, Bathymetry of the continental rise off Cape Hatteras: Deep Sea Research, vol. 14, p. 625-633.

Shepard, F. P., and Dill, R. F., 1966, Submarine canyons and other sea valleys: Rand-McNally, Chicago, 381 p.

Stacey, J. R., 1958, Terrain diagrams in isometric projection-simplified: Ann. Assoc. Amer. Geog., v. 48, p. 232.

Uchupi, E., 1966, Maps showing relation of land and submarine topography, Nova Scotia to Florida: U. S. Geol. Surv. Geol. Invest., Map 1-451, 3 sheets.

SURGE FLOW: A MODEL OF THE WALL LAYER

By

William F. Tanner
Geology Department
Florida State University
Tallahassee, Florida

ABSTRACT

Thin sheets of flowing water have been studied on various inclined surfaces, including smooth glass, asphalt, concrete, wood, loose sand and fixed sand grains. Flow was accompanied by more-or-less regular surges (also described by different workers as roll waves, rain waves, slug flow and kinematic waves). Controlled variables were slope angle, discharge, surface roughness, surface tension and viscosity. Surges initially constitute an almost-random phenomenon; they are quickly modified by surface tension and other effects and become regular in geometry and speed.

Similar features have been studied in the thin wall layer in a smooth-bottomed tilting flume. Surface tension effects do not apply under water, but the surface surges are nevertheless thought to be thin-sheet counterparts of transverse banding in the wall layer. In thin sheet flow, over rigid beds, the water-air interface is easily deformable, and the bed is not, hence surges form at the water surface. In the wall layer, between deep water and a mobile granular bed, bed shear is increased by a factor of 10 to perhaps 10^4 times and subtle deformation of the bed is thought to result. The very low shear ridges, which actually appear under water on sand beds before individual grain motion is visible, are thought to be caused by the wall layer equivalent of thin sheet surge flow. Such ridges, once formed, require an almost instantaneous development of water bottom eddies, which in turn shape the ridges into ordinary sub-aqueous ripple marks.

If this identification is correct, a form of surge flow in the wall layer is responsible for initiation of sediment particle motion. Reynolds and Froude numbers based on wall layer thickness are generally in the ranges of $R = 10$ to $R = 10^3$, and $F > 1.0$; work with tracers also indicates that the regime in the wall layer is laminar but rapid. This work suggests that initiation of sediment motion is a Froude phenomenon; once sub-aqueous ripple marks have developed, continuation of sediment transport is a Reynolds phenomenon.

Observation of natural thin sheet flow, over mobile granular beds, shows that any one of the several Froude regimes can form the sand surface markings which may be preserved in the rock record. It is not necessary to reason that, as the water velocity drops, only a

ripple mark field can be left behind. This observation may explain smooth horizontal surfaces described from lithified counterparts, and perhaps even certain traces of rapid flow.

INTRODUCTION

Rain waves are extremely common on dirt and on paved or black-topped surfaces having gentle to intermediate slopes. These waves typically occur in water, a few tenths of a millimeter to about a centimeter deep, and appear as asymmetrical ridges oriented transverse to the direction of flow. Unlike standing waves, which develop commonly in deeper water when the Froude number exceeds $F = 1.0$, they move with considerable celerity, travelling faster than the surface water itself, and they may be accompanied by much smaller capillary waves ahead of the crest and steep slope.

Several terms have been used to describe these, or similar, features: slug flow (Mayer, 1957), roll waves (Koloseus and Davidian, 1966),kinematic waves (Lighthill and Whitham, 1955), surge flow, rain waves, and others. The waves themselves have been observed in both natural settings (rain waves; surge flow) and the laboratory. Because similar features develop in deep water, a general term, such as surges, or kinematic waves, is needed. The term "surge" has been adopted in this paper, pending greater clarification of differences between the supposed varieties.

I have been interested in surge flow for several years, and have carried out a series of systematic observations and experiments since early 1965. Surge flow (in the thin sheet sense used here) occurs naturally on flat-bottomed, sand floored creeks and canals, as well as on more-or-less rigid surfaces such as concrete and asphalt. I have studied laboratory examples (on slopes from less than 1° up to 60°) and natural occurrences.

Mayer (1957) distinguished between "roll waves" and "slug flow" in several ways, based on fluid behavior, position in an experimental flume and Froude number. Rain waves observed in streets were characterized by Mayer as roll waves, having high vorticity in the crests, and quiescent troughs; slug flow, on the other hand, was described as consisting of turbulent ridges separated by highly agitated regions. Mayer further specified that roll waves form only between the limits $1 < F < 2$ (where F is the Froude number) and that slug flow develops only at Froude numbers greater than 2. I have been unable to make a distinction between roll waves and slug flow.

Acknowledgments

Gratitude is hereby expressed to Clemson University for permitting use of their hydrodynamics laboratory, and to Bruce Tanner,

who was an able assistant throughout much of the flume and thin sheet experimentation.

PROCEDURE

Natural rain waves during run-off following rain were observed on asphalt street surfaces inclined as steeply as 8° and on concrete surfaces as steep as 60°. Natural surge flow was studied in channels floored by loose sand. Excellent examples were seen in creeks where little or no binding material (i. e., clay or organic matter) was present in the sand, and hence a braided pattern was maintained; the presence of many channels did not hinder the development of surges.

Flume work was carried out at Clemson University, in a tilting flume maintained by the School of Agriculture. Controlled thin sheet flow was studied at Florida State University on various surfaces, including wood, glass, silt cemented on glass and sand cemented on glass or wood. Factors which were varied in most of these experiments were slope angle, discharge and roughness. A small number of tests was run in which surface tension and viscosity were altered.

The most important measuring instrument has been a millisecond timer operated by finger-tip remote control. Velocities were readily obtained over a measured course; five to ten readings were averaged for each data point, and the resulting figure was taken to 0. 1 second. Crest spacing was obtained by combining velocity with elapsed time between two successive crests, a procedure which appears to be more accurate than making simple linear measurements of a moving form. Spacing was considered to be accurate to one centimeter or less; in some of the early work, before the timer was put to this use, spacing data were not as accurate.

Water depth was measured between the surges, with a thin centimeter stick held so as to present minimum resistance to the flow; this method was adopted for thin-sheet flow because there were no walls on which depth markers could be placed. Depth measurements were accurate to 0. 05 cm at depths of 0. 1 cm or greater. Discharge was monitored at regular intervals, but was not measured continuously; the variability of this factor appears to have been small. No discharge measurements were obtained for natural flows, or even for all of the laboratory experiments.

Capital letters (B, C, R, S, etc.) have been used to designate series of experiments which differed from each other in some significant way; i. e., the C series of experiments indicates those run in relatively deep water (7 to 20 cm depth) in a flume (Table 1).

Table 1. Summary of Experimental Work.

Series	Runs	Depth	Mobile Bed	Setting	Surface	Slope	Discharge
C	13	7-20 cm	No	Flume	Smooth	0-1.67°	Constant
B*	11	0.2-2 cm	No	Sheet	Smooth	10-60°	Varied
D	9	0.01-0.1 cm	No	Sheet	Varied	4.5-21°	Constant
E	7	0.1 cm	No	Sheet	Smooth	10°	Varied
S	5	0.1-2.0 cm	No	Sheet	Rough	2-8°	Varied
H	16	0.01-0.1 cm	No	Sheet	Varied	1.3-12°	Varied
J	12	~ 0.05 cm	No	Sheet	Varied	6.5-23°	Varied
R	2	0.2 cm	No	Sheet	Rough	2-60°	Varied
M	20	0.1-2 cm	Yes	Creek	Rough	> 1°	Varied

*The B series included one specific set of circumstances, duplicated several times, using oil instead of water; and several runs were duplicated using reduced surface tension.

GEOMETRY

Surge crests begin to develop within a few centimeters or tens of centimeters of the upper end of the experimental plate. They are initially small, close together, ragged in outline, have discontinuous crests and exhibit a wide range of velocities. Within a few seconds the dominant forms emerge, and the pattern tends to become quite regular, except where changes in slope or roughness require modifications in depth or velocity, or both. The crests become straighter and longer as adjacent forms merge, but generally show frictional retardation (and hence curvature) near the edges of the flow.

The crests are typically a few tens of centimeters apart and asymmetrical in profile, with the steeper slope facing down-current. The water depth is commonly between 0.005 cm and 1.0 cm, with a variability between trough and crest on the order of a factor of two to four.

Although the Froude number (defined in a subsequent section) for the surge flow regime is greater than F =1, there has been no evidence, in flow over rigid beds, of surges and other waves forming at the same time, or appearing simultaneously in the same reach. On a mobile bed, however, surges have been observed passing systematically through a field of antidunes, where the Froude number was close to 2.

The maximum spacing observed between crests has been about 8 meters, in a natural flow on loose sand, and the minimum about 3 cm, on a clean smooth glass plate. These are all "long" waves, with spacing markedly greater than height; typical values of the spacing-to-height ratio were between 150 and 300.

When the surface tension was reduced by using a commercial detergent (Photo-flo), the spacing between crests increased greatly, and there was a small decrease in crest celerity. The only tests of the effects of surface tension were made at a slope angle of 40°, with approximately a three-fold increase in the crest spacing and about a one-third reduction in the celerity. It appears obvious that part of the geometry of a surge system is due to surface tension, but a slip-stick-slip mechanism of some kind, deemed originally responsible for the surges, also operates under deep water, and therefore cannot be a surface tension effect.

Dye tracers in very shallow water show that after surges are well developed, the flow moves in two layers. An upper layer of flow contains the surges, and the lower layer does not. The bottom layer is about as deep as the original flow in which the crests first developed; the top layer is discontinuous and is made up of well-spaced crests. Capillary (or shock) waves, ahead of each crest ridge, are taken as evidence that the upper layer moves relative to the lower. Crest spacing, in a limited number of trials at 40°, appears to have been proportional to viscosity.

DIMENSIONLESS CRITERIA

The Reynolds number contains in its formulation a representative length. This length is commonly taken as the water depth, although such a practice certainly cannot be defended when one is dealing with the deep ocean or the atmosphere, nor is the depth of water (even in shallow streams) really the same kind of length as pipe diameter, originally used by Osborne Reynolds. For a settling grain, the representative length is some measure of the grain diameter. For bed roughness, the representative length may be a spacing of some kind, such as the wavelength of ripple marks, or the average distance between sand bars, or it may be a representative grain diameter.

In a single flow, all of these different kinds of lengths may be present. There is, therefore, a spectrum of lengths, all of which may be pertinent parts in the geometry of the system. Because these may be independent of each other, no single length can be used exclusively in computing the Reynolds number.

With the exception of the M series of experiments, none of the experiments reported here involved mobile bed materials, and hence grain diameters and bedform spacings have not been pertinent to most of the work. Instead, two measures of length have been adopted: water depth, d, and surge spacing, λ (= wave length). In the thin sheet tests, the Reynolds number based on depth, R_d, ranged from 10 to 10^3. The use of dye has verified the impression that general turbulence does not exist at such low Reynolds numbers. There is, however, local turbulence near some of the surge crests.

The Reynolds number based on wave length, or spacing, R_λ has been above $R_\lambda = 20,000$ for thin sheet flow. In a general way, both Reynolds numbers increase with slope angle, and both increase with discharge, which is to be expected inasmuch as each is a direct function of velocity. However, the relationship is not clear enough for either one to be predicted from the other.

The Froude number also contains a representative length in its formulation ($F = v/\sqrt{\gamma l}$, where v = velocity, gamma is the acceleration of gravity, and l is a length).

For this parameter, also, a spectrum is indicated. For reasons stated above, only F_d and F_λ have been used in the present study.

With the exception of six questionable values in the range $F_d = 0.3$ to $F_d = 0.8$, all results obtained for this parameter have been greater than $F_d = 1.0$; the questionable values depend on depth measurements, which have been difficult to make in some instances. The spacing parameter F_λ has fallen in the range $F_\lambda = 0.11$ to $F_\lambda = 0.91$.

The two Froude numbers show a much closer mutual relationship than do the two Reynolds numbers. For one series of experiments with constant bed slope, and varying discharge, F_d was rather close to ten times F_λ, and both increased with discharge. Each Froude number is also directly proportional to the slope angle. Both of these observations should follow from the fact that velocity, which responds readily to changes in discharge and slope, is the most important measure contained in the Froude number as ordinarily defined.

The ratio of the two parameters, F_λ / F_d, increased directly with surface tension, and decreased with an increase in fluid viscosity, in the short series of experiments designed to test the effects of these two properties.

One of the most useful plots (Figure 1) obtained in the course of the study used a Froude number as one ordinate and a measure of the slope angle as the other ordinate. For each series of experiments, as a single variable was altered, an essentially straight line was obtained. For the entire study, however, it is clear that not all results are replicable, and that at least one important variable, perhaps surface roughness, has not yet been properly defined. This observation holds true even for successive experiments on supposedly identical glass plates.

In general, the ratio i/F_λ, where the slope angle i is measured in radians, has been close to 0.5 in flume experiments (the C-series), between 0.5 and 2.0 in thin sheetflow on smooth glass and on roughened glass, and between 0.5 and 4.0 in the thin sheet flow on surfaces such as asphalt and concrete. Increased viscosity, or reduced surface tension, increases the value of this ratio. The choice of F_λ, rather than F_d, is based on the fact that spacing is much easier to measure, relatively accurately, than is depth, especially as the latter becomes small. The variability that remains, in thin sheet flow of ordinary water having the usual values for viscosity and surface tension, is

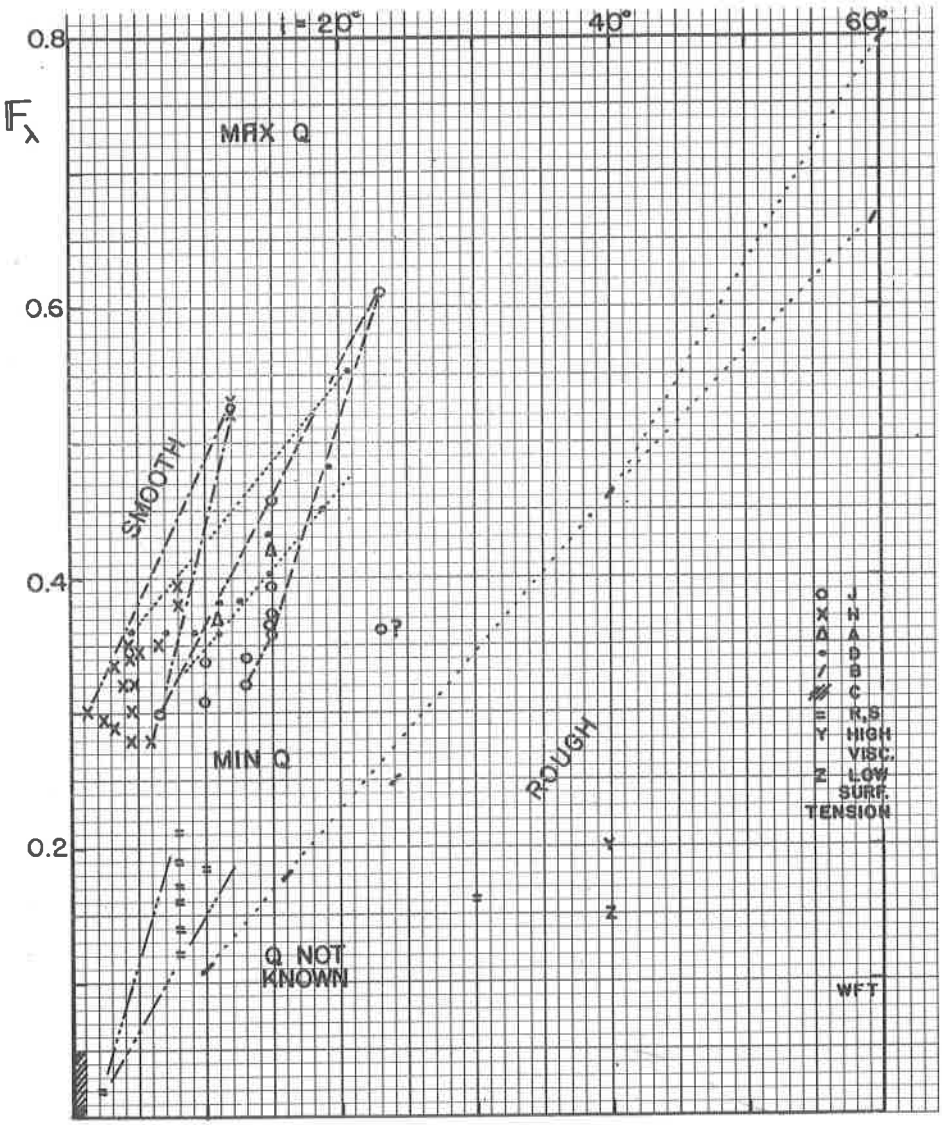

Figure 1. Selected results plotted in terms of $F\lambda$ (Froude number, based on wave-length, or spacing) and i (slope angles). The key is given along the right-hand margin. C results represent a series of runs obtained in the Clemson University tilting flume. R and S results were obtained from natural rain waves on asphalt surfaces, except for the point i = 30, taken on concrete. The B series was designed primarily to extend data to large slope angles. Several sets of experiments were run with constant slope, and hence are not shown here; data points falling very close to each other have also been eliminated. In general, each set of data falls within a band which slopes upward to the right (that is, F varies directly with i).

largely due to discharge, which affects F_λ directly without altering i, and to a much less extent to a roughness factor which is as yet uncertain.

Most of the work described here has been carried out at angles between 1° and 60°, with the bulk of the data between 3° and 25°. Measurements taken at angles below about 8° have proven to be much less reliable than those at higher angles.

The C-series (observed in the flume) produced results, computed from total water depth and maximum water velocity, of R_d between 2,600 and 23,500, and F_d between 0.017 and 0.1; in the wall layer, however, interpolated values are higher for F and lower for R. The wall layer is identified, in the C-series, as that layer in which $F_d \geq 1.0$; this identification is made, as a working hypothesis, in order to compare some part of the flume flow with thin sheet behavior. Thickness of the wall layer, computed from this assumption, ranged from a low value of d = 0.003 cm to a high of d = 0.04 cm (based on velocities in the range of 1 to 7 cm/sec). Reynolds numbers computed for this depth were between R_d=0.005 and R_d=0.24. There was no general turbulence near the bed of the flume, and local turbulence was mild and rare.

Bed activity, similar to surge flow in thin sheets of water, was exhibited in most of the runs. This consisted of development of parallel bands of dye, transverse to the direction of flow, in the bottom few millimeters of water, where dye was injected to form sheets; or intermittent motion of single light particles on the bed, with an average particle "jump length" of close to 20 cm (minimum observed, 12 cm; maximum observed, 30 cm).

PREVIOUS RESULTS

Koloseus and Davidian (1966) obtained slightly different results. They used water depths more than 10 cm, and angles below 4 degrees; they reported no roll waves (surges of the present study) in water less than about 1.2 cm deep. They also observed no roll waves closer than about a meter from the point of origin, whereas the present study typically obtained surges within 10 to 20 cm of the origin.

Lighthill and Whitham (1955) reviewed kinematic waves in general, and used as examples "flood waves" on long rivers as well as traffic jams on roadways. They pointed out that, in the case of rivers, each wave crest contains more water than adjacent reaches do, and that the velocity depends on this fact. This requires that kinematic waves travel faster than the water in the reaches between crests, and further that larger waves overtake smaller ones. This mode of behavior produces a fairly regular train of waves, each of which is close to the optimum size and travels at an optimum velocity. Lighthill and Whitham considered such kinematic waves to be shock waves.

The surges described in the present study constitute a class of kinematic waves. They obey the same general requirements specified by these two authors, the larger ones travelling with greater velocity than the smaller ones, thus producing a regular train. They have steep forward slopes, and are typically preceded by a short train of capillary ripples on the water surface; this observation is evidence for the shock, or overriding, nature of the wave front. The shock wave front is a discontinuity between velocity and depth values for immediately adjacent parts of the flow.

Lighthill and Whitham thought that their roll waves appear only when the Froude number exceeds F = 2. This restriction does not hold in the results described herein.

Binnie (1957) attempted to determine the minimum Reynolds number at which roll waves first form, using a vertical glass surface. He cited results from earlier workers, ranging from R = 2 to R = 6.25, and obtained in his own experiment R = 4.4. Benjamin (1957) ventured the opinion that undamped waves exist at all finite values of R, and that therefore, no critical R exists. He cited previous work in which roll waves were described with R = 1.5.

Minimum Reynolds numbers obtained for surge flow, in the present study, have varied from one series of experiments to another. In the flume work, a systematic discontinuous jumping motion of sediment particles appeared with computed values as low as $R_d = 6$. (The term "saltation" has been avoided deliberately.) In the E series (constant slope; i = 10°) the minimum Reynolds number was $R_d = 200$, with minimum discharge per unit width.

In the H series minimum R was $R_d = 230$, at i = 8°; other runs in the same series were made at angles ranging from 1.3° to 12°. In the D series, R varied between $R_d = 60$ and $R_d = 180$, with the minimum value computed from data at an intermediate angle (i = 11°). A "minimum" Reynolds number does not appear to exist.

FROUDE MARKS ON SAND

Observation of natural thin sheet flow over loose granular beds shows that the high-Froude regime, observed under similar conditions in the laboratory, is not an artifice. Under natural conditions where either evaporation, or infiltration into the bed, or both, is reducing the discharge per unit width, the decrease in depth in the downstream direction may be sufficiently great that the Froude number, F_d, does not drop below unity, despite a concomitant reduction in velocity. The bed shear, under these conditions, is so small that sand grains no longer move (except locally), features which are left on the dry bed may have been inherited from any one of the several Froude regimes. That is, a plane bed may be left, in this fashion, if the ambient value of the Froude number was close to 0.7 when grains were last moving; and

evidences of rapid flow may be left if the ambient value was greater than 1.0 when grains were last moving. These observations of natural flow conditions show that it is not necessary for the bed to be left in a ripple marked condition; they may, further, provide an explanation for smooth sand surfaces which have been described from lithified equivalents.

Sandy beds on which water flow decreases, as described above, are fairly common, hence evidence of more than one Froude regime should have been preserved in the rock record. The dearth of reported examples may arise from the possibilities that either geologists do not normally know to look for high-regime markings, or geologists with a background in hydrodynamics "know" that such markings cannot be left on a sand bed. Smooth sand surfaces, fairly well known from the stratigraphic section, should be studied more carefully, in an effort to determine whether or not they may have been formed by transition-regime flow.

WALL LAYER

In most of the experiments, there has been very little turbulence. For the H-series of tests, for example (in which the slope angle was varied between 1.3° and 12°, and the discharge-per-unit-width was varied between 2.365 cm^2/sec and 5.258 cm^2/sec), the Reynolds number, based on the usual assumption that water depth is the representative length, fell in the range $R_d = 230$ to $R_d = 580$. For the J-series, with slope angles between 6.5° and 23°, and discharge-per-unit-width between 1.78 cm^2/sec and 2.15 cm^2/sec, Reynolds numbers fell in the range $R_d = 190$ to $R_d = 450$. The C-series of experiments, in which water depths were as great as 20 cm, produced Reynolds numbers as high as $R_d = 23,500$ and as low as $R_d = 2,600$, using the entire depth as the representative length.

The Reynolds number, as generally defined, is

$$R = v \ell \rho / \psi$$

where v = velocity, ℓ is a length, ρ is density, and ψ is dynamic viscosity. R is thought by engineers to have a critical value near 3,000 or 4,000 in pipes, separating laminar flow (lower numbers) from turbulent flow (higher numbers). Work with motion in unconfined systems, however, shows that the pipe-criterion is much too high (Tanner, 1963a, 1965), and indeed several different critical values probably exist. That is, in natural flow, one encounters a spectrum of critical values, the numerically smallest approaching R = 1 and being a measure of turbulence in the vicinity of a grain. This would be properly defined as $R2_r$ where the diameter (that is, twice the radius) is the representative length.

Nevertheless, the R_d values obtained in thin-sheet flow were all in the range $R_d = 60$ to $R_d = 1,000$, and general turbulence was present

in no single instance. In flume experiments (the C-series), turbulence was also not general, although it was present locally.

The boundary layer thickness, δ, is commonly computed as the thickness of that layer of flow in which the velocity does not exceed 0.99 of the maximum flow in the system. In the thin sheet experiments, no layer of water is at any great distance from the bed (water depths have been, generally, between 0.01 and 1.0 cm), and hence velocities at all points have been reduced more or less by drag. Consequently, it becomes important to obtain the boundary layer thickness in some other way. A widely used procedure depends on the relationship

$$\delta = (x/U)^{0.5}$$

where x is the distance, in the direction of motion, from the initiation of the flow pattern, and U is the water velocity. In the H-series, for example, where water depths ranged from a minimum of about 0.05 cm to a maximum of about 0.1 cm, the computed thickness of the boundary layer was 1.1 to 1.94 cm. In no case was the computed boundary layer thickness as small as six times the actual depth.

The wall-layer thickness, Y, is generally held to represent a layer, immediately adjacent to the wall, no thicker than 1/7 the boundary layer thickness (Rouse, 1959, p. 346). Using the computed boundary layer thickness of 1.1 to 1.94 cm, one obtains a range of maximum wall layer thicknesses of 0.157 to 0.277 cm. In the D, E, J and H sets of experiments, no water depth exceeded 0.15 cm. In the B, R, M and S sets, thin sheet water depths were as great as 2.0 cm, but much longer beds were used, and the actual water depth was in no instance as large as 1/6 of the computed value for the boundary layer. It is concluded that the thin sheet work is essentially a study of the bare wall layer (that is, the wall layer without additional water above it).

In the C-series a flume was used, and water depths were as great as 20 cm, but the region of prime interest was that layer, 1 cm thick or less, closest to the bed.

The most obvious characteristic of the thin flowing sheets described here has been the surges; these are primarily geometrical in nature, and therefore cannot be studied very well in a deep flume.

Because little or no turbulence appears in the wall layer, one is justified in interpolating velocity, as a first approximation, from v = U at the water surface to v = O at the bed. Highly precise measurements, not undertaken in this sequence of experiments, may ultimately modify this approximation somewhat, but the changes should not be very great. In the flume experiments, velocity measurements closest to the bed were taken at heights above the bed of 0.1 to 0.5 cm. Velocities obtained at, for example, 0.1 cm, 9 cm, and 18 cm (Run C-3), were 1.72, 2.00 and 2.38 cm/sec, respectively. These results plot, on coordinate paper, as a straight line, supporting the interpolation procedure.

In analyzing the C-series data, a straight-line plot of velocities was extrapolated downward to that place where the Froude number

based on depth, F_d, was equal to 1; from here, the plot was extended to v = O precisely at the bed. This procedure produced inflection points in the neighborhood of 0.1 cm above the bed. The conclusion was therefore drawn that the lowest millimeter of water, in the flume tests, was behaving approximately as the entire water mass in the thin sheet experiments. (The justification for using $F_d = 1$ as a criterion is presented under another sub-heading).

If thin sheet flow is actually the bare, or stripped, wall layer, experiments with such flows may shed a great deal of light on processes which take place close to the bed in natural bodies of water. Detailed development of the several experimental series, which have been carried out, has been based on this probable identity.

The computed thickness, δ, of the projected boundary layer, fell in the range 1.1 to 1.94 cm for the H-series. Faller and Kaylor (1966) observed "shear-induced vortices" in which the spacing was 11 times a characteristic depth which they calculated from kinematic viscosity and a rate. Early in the present experiments I deduced a relationship of $\lambda = 14$ d, which I later began to doubt. In the light of the report by Faller and Kaylor, I calculated a "forecast" value for the wavelength, or spacing (despite the obvious differences between the two investigations), using the formula $\lambda = 11d$. For the H-series, for example, this produced a range of values for spacing from 11.2 to 16.3 cm. Observed values for the same series ranged from 11.48 cm to 22.45 cm. The departures, per experiment within the H-series, ranged from a low of 0.3 cm to a maximum of 5.8 cm (using constant discharge but varied slope), with an average departure of the computed spacing from the observed spacing, of 2.35 cm.

A computed water depth can be obtained from this relationship, rewriting it in the form

$$d < 0.013\lambda ,$$

which is based on the limiting value of $d^{-1} = (11)(\lambda)$. This approach to water depth appears to provide very good limits at low slope angles (i.e., 3° and less), but not so good at steeper slopes.

SHEAR

Computations were made for total shear stress ($\tau = \mu dU/dy$), bottom shear stress ($\tau_o = W_s ih = g\rho ih$, where i is the slope angle, h is the hydraulic radius or depth, ρ is fluid density, and g is the acceleration of gravity), and the shear velocity ($U_* = \sqrt{\tau/\rho}$). The last of these is a function of fixed values (acceleration of gravity, water density, slope angle) and a nearly-constant value (depth), and hence cannot vary much, unless the controlling conditions are varied. It is not surprising, then, that a plot of i vs U produces a very nearly linear arrangement.

Bottom shear stress, τ_o, is also a function of fixed values, of

which only one (slope) can be controlled, with only one uncontrolled variable (depth); accordingly a suitably designed plot of τ_o vs i is also very close to a straight line.

The variability of these two parameters is, however, more than might be desired. This may be due in large part to the fact that the only uncontrolled variable in either one (water depth) is extremely difficult to measure in thin sheet flow. For the experiments run with water (all except part of the B-series), the fluid density is $\rho \sim 1$, and $U_* \sim \sqrt{\tau_o}$. The bottom shear stress, τ_o, being the larger number, will show a greater numerical variability, and hence is reported here. In thin sheet flow, τ_o was between a minimum value of 3.3 (i = 1.3°) and a maximum of 170 (i = 60°). Most of the experimental work was done with τ_o in the range 3.3 to 20. Natural rain waves (R and S series) had values between 3.4 (i = 2°) and 102 (I = 60°; rain waves on a concrete slab adjacent to a bridge) (τ_o values in g/cm-sec^2).

In the flume experiments, τ_o was much higher than the bed slope would have indicated, based on thin sheet experiments: 66 to 167. Apparent surge-type activity on the bottom (transverse bands of disturbed fluid; systematically intermittent transport of single particles on the bed) took place generally when τ_o was below about 70. Part of the difficulty with comparing wall-layer observations, in a flume, with thin sheet flow is associated, as is stated in more detail in another section, with the difficulty in measuring velocities in the flume close to the bed (i.e., at 0.01 cm) and in measuring depths in the thin sheets. A further difficulty may be associated with bed roughness effects.

The total shear stress, for all runs except a viscosity test as part of series B, is a direct function of the velocity gradient. It therefore is not controlled in a closely-coupled fashion, as τ_o and U_* were, by slope angle. The total range of values obtained, for thin sheet flow, in gm/cm-sec^2, was 100 (at a relatively high angle, i = 10°) to 1,360, with a single erratic result of 1,800 (also at a relatively high angle, i = 23°, but definitely not near the maximum angle used, i = 60°). Values from the flume runs occupied the range from 160 to 740. Natural rain waves (R and S series) were spread from 200 to 1,000. The smallest values (from the B series) was 100, from thin sheet flow in an oil having a measured viscosity of 160 cp. The shear stress computed for the flume wall layer, only, was between 77 and 280, about the bottom of the overall range.

Because the velocity gradient in the thin sheet between crests must be essentially rectilinear at any given moment and bed location, U/y has been used in lieu of dU/dy, with U = O at y = O. This means that, even with the assumption of linearity, any calculation of τ is highly sensitive to errors in measuring water depth. As a result, a plot of τ vs Q/w (discharge per unit time per unit width of flow) may show a great deal of scatter. Nevertheless, in the three series which were designed to test a possible relationship here (E, H, J), certain results are clear. The shear stress increases with the slope angle (at 13° and

15°, values were between 1,000 and 1,200; at 4.5°, between 300 and 520). The shear stress also increases with the discharge per unit width, with the results being clearer at low angles (velocities are lower and depths are greater and hence easier to measure) than at high angles. These are, of course, results which might have been anticipated.

OTHER RESULTS

The gravest difficulty encountered throughout the program was the measurement of water depth. Because this problem was never solved satisfactorily, many data plots show more scatter than they should. Nevertheless, reasonably clear relationships have emerged from the observations.

On a plot of slope angle (i, in radians) against velocity, most of the data cluster in a fairly narrow belt which can be represented approximately by

$$v = 143i + 25$$

where velocity is measured in cm/sec. Velocity in thin sheets is, however, strongly sensitive to discharge, and somewhat sensitive to roughness. The flume data cannot be included in such a representation, inasmuch as deep flow cannot be maintained in a flume, at high slope angles, whereas thin sheet flow is easy to maintain at high angles.

In one graph, fixed factors, iQ/w (that is, the product of slope angle, in radians, with discharge per unit width) were plotted against variable or response factors, λv (that is, the product of crest spacing with velocity) (Figure 2). Most of the data plot along a line which can be represented as

$$wv\lambda / iQ = k$$

where k is dimensionless and has the approximate value of 3250. The largest departures from this line were obtained as a result of increasing roughness. In general, i can be seen to increase with both λv and iQ/w (which it should, of course) but Q has a maximum near $\lambda v = 900$ and $iQ/w = 0.3$, (λ in cm; v in cm/sec; Q in cm^3/sec; w in cm) with reduced discharges falling toward the ends of the line. These results are particularly useful, in studying thin sheet flow, because each of the measurements is relatively easy to obtain in laboratory experimentation where Q can be metered fairly accurately. In studying natural rain waves, however, Q must be computed from depth, which reduces precision accordingly. Hence natural rain waves are not as useful as is laboratory experimentation.

SEDIMENT TRANSPORT

Most of the thin-sheet experiments have been run on rigid surfaces, where no loose grains of sediment were available for transport.

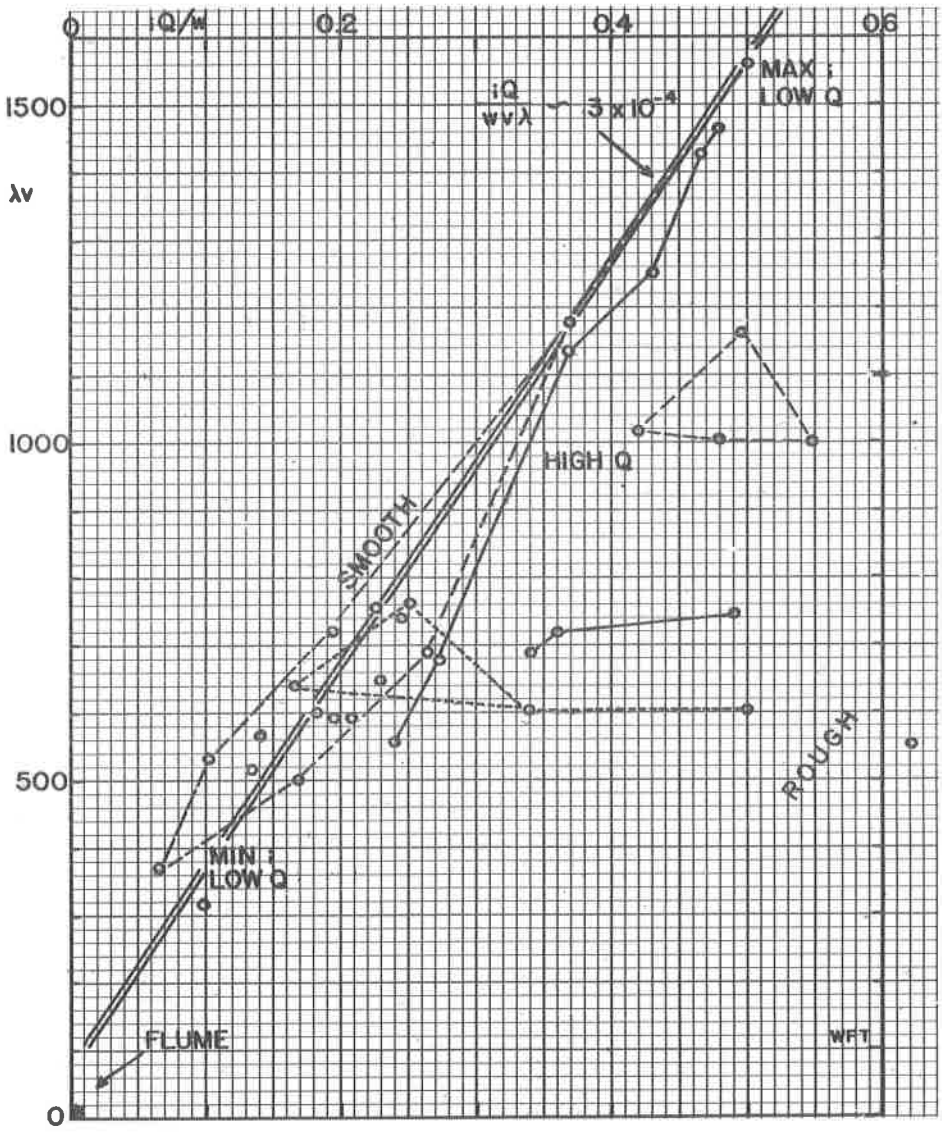

Figure 2. Selected results plotted in terms of iQ/w (slope angle; discharge per unit width of flow) and λ v (wave-length, or spacing; velocity). Measurements obtained from a single set of experiments are connected by or enclosed within, single straight lines (either solid or dashed). Where roughness effects were being studied, related data points may lie on more-or-less horizontal lines; where discharge, slope and velocity were being studied on smooth or nearly smooth surfaces, related data points lie on lines or bands which slope upward to the right (that is, λ v varies directly with iQ/w).

The only surface which could be deformed by flowing water, was the upper, or air-water, surface. A few observations have been made of thin sheet flow on loose sand; because total water depth is typically less than a centimeter, pressure on the bed is small (i.e., 0.1 g/cm, in excess over atmospheric pressure); even though the bed is mobile, the upper surface (against air) is much easier to deform. As the water depth is increased, this differential between the two surfaces of the wall layer is reduced.

The bed shear (τ_o) computed from the flume data (water depths up to 20 cm) was 30 to more than 100 times as great as the bed shear obtained from thin sheet flow at closely comparable angles. In the wall layer on a river bed, the factor might be 10^3 or 10^4. The upper surface of the wall layer is still deformed, at certain velocities under deep water, but a mobile bed is also much more likely to be deformed. Obviously a small ridge, or step, created in the mobile bed, cannot be swept downstream as rapidly as surges can move over a thin film of water; nevertheless the presence of such a bed surface dislocation contributes, in turn, to other processes which tend to move individual grains. Bagnold (1956) previously discussed the role of tangential stress in moving sand grains.

From the experiments described here, and wave-tank and related work performed earlier (Tanner, 1963b), the tentative conclusion is drawn that surge flow, in the wall layer, is responsible, when the velocity is high enough, for the formation of shear ridges in the mobile bed material. These subtle ridges, in turn, require the development of eddies having axes which are horizontal and normal to the direction of flow. The eddies amplify the shear ridges, building them up into sub-aqueous ripple marks. The flow patterns which arise, at this point, differ under unidirectional flow (i.e., in river channels, canals and flumes) and under oscillating flow (wave action in lakes and seas). In the latter case, each wave-driven bottom orbit is underlain by eight to about fifteen cells, each of which is composed of two components like a figure eight; these reverse direction from one end of the "eight", to the other, with each wave passage. As a result, some 15 to 30 ripple marks are maintained under each wave length. In the former case, there is no systematic reversal of direction, and instead the individual eddies begin to tilt, break up and decay. In both cases, however, there is an acceleration up the up-current slope, on each ripple mark, and a rain of sediment particles onto the down-current slope and into the adjacent trough. At this stage, individual sediment grains may make regular jumps having lengths approximately equal to one half the wave-length, or spacing, of the ripple marks. An increase in water velocity can then easily convert the "rain" of grains into a true turbulent suspension.

A previous set of experiments (Tanner, 1967) was designed to show that a systematically applied shear, on a sheet of loose sand, can and does produce a system of parallel ridges which lack only amplitude

to duplicate ordinary subaqueous ripple marks. The model which was used in those experiments incorporated no turbulence, and hence did not provide the necessary amplitude. The subtle shear ridges which were formed, however, appear to match -- in every detail -- the ridges produced on a smooth granular bed by the first two or three strokes of a wave generator (that is, before eddies have developed).

The surge flow experiments suggest a mechanism whereby such ridges can be formed under moving water. Not only does it appear that thin sheet flow reproduces important features of the wall layer, it also appears that surge flow on thin sheets (i. e., roll waves or rain waves) illustrates the mechanism which, in the wall layer, is responsible for the initial subtle deformation of the mobile bed which, in turn, leads to ripple marks and sediment transport.

CONCLUSIONS

Regularly-spaced surges appear on thin flowing sheets of water at Reynolds numbers (R_d) between 6 and 1, 000 (laminar or transitional range), and at Froude numbers (F_d) greater than 1 (with a few questionable exceptions; the rapid or shooting regime).

The thin sheet of flowing water has been investigated as a possible model of bare wall-layer flow. There are obvious objections to this comparison; for example, surface tension is an important factor in controlling the geometry and velocity of surges, a factor which cannot operate in a true wall layer along the bed of a channel. Nevertheless, surface tension can only modify a feature which is already present, hence the measurements obtained describe a phenomenon which appears to take place in the wall layer, where it is modified in one way, as well as in thin sheet flow, where it is modified in a different way. A slip-stick-slip mechanism of some kind is thought to be responsible for wall layer banding, in deep flow, and for surges in thin sheet flow.

The same mechanism is thought to be responsible for ripple marks (Tanner, 1963b), in a system where these bed forms set up a special form of eddying which in turn modifies the current or wave regime near the bottom. In each of these instances, it is thought that some other process imposes a regularity on the almost-random nature which is visible in the first second of surge development. For thin sheet flow, the main modifications are the work of surface tension.

A somewhat different approach to the same phenomenon has been provided by Brandt and Bugliarello (1966). Both sets of results are pertinent to any study of the entrainment of sand grains in moving water.

The regularities which have begun to emerge from the numerical data are, in a way, self-negating. This is true because maximum regularity is found only at relatively great distances from surge initiation; those measurements taken closest to the source tend to have the greatest scatter. This, in turn, leads to the implication that the

inferred slip-stick-slip mechanism, prior to modification, is of a highly varied nature, statistically. However, most granular beds are not close to the upstream point of "surge" initiation, and therefore the regularly spaced surges (or roll waves) which can be observed so commonly in nature, are taken as a good model of wall layer banding, which in turn causes subtle shear ridges in mobile sediment.

REFERENCES CITED

Bagnold, R. A., 1956, The flow of cohesionless grains in fluids: Royal Soc. of London, Philosophical Trans., Series A, v. 249, p. 235-297.

Benjamin, T. B., 1957, Wave formation in laminar flow down an inclined plane: Jour. of Fluid Mechanics, v. 2, p. 554-574.

Binnie, A. M., 1957, Experiments on the onset of wave formation on a film of water flowing down a vertical plane: Jour. of Fluid Mechanics, v. 2, p. 551-553.

Brandt, A., and Bugliarello, G., 1966, Concentration redistribution phenomena in the shear flow of monolayers of suspended particles: Trans. Soc. Rheology, v. 10, p. 229-251.

Faller, A. J., and Kaylor, R. E., 1966, A numerical study of the instability of the laminar Ekman boundary layer: Jour. Atmos. Sciences, v. 23, p. 466-480.

Koloseus, H. J., and Davidian, J., 1966, Free-surface instability correlations: U. S. Geological Survey, Water Supply Paper 1592-C, 72 p.

Lighthill, M. J., and Whitham, G. B., 1955, On kinematic waves: I. Flood movement in long rivers, Royal Society London, Proceedings, Ser. A., v. 229, p. 281-316.

Mayer, P. G. W., 1957, A study of roll waves and slug flows in inclined open channels: Ph.D. dissertation, Cornell University.

Rouse, H., ed., 1959, Advanced mechanics of fluids: John Wiley and Sons, New York, 444 p.

Tanner, W. F., 1963, The scaled-UP model in studies of sediment transport: Bull. American Assoc. Petroleum Geologists, v. 47, p. 372.

Tanner, W. F., 1963, Origin and maintenance of ripple marks: Sedimentology, v. 2, p. 307-311.

Tanner, W. F., 1965, Spiral motion, sediment transport, and river development: Proc. Fed. Inter-Agency Sediment Conference, 1963, U. S. Dept. of Agriculture, Misc. Public. No. 970, p. 330-335.

Tanner, W. F., 1967, The ripple mark analog: preliminary results. Southeastern Geology, v. 8, p. 67-72.

STRUCTURAL FEATURES OF THE COASTAL PLAIN OF GEORGIA

By

Howard Ross Cramer
Emory University

ABSTRACT

Twenty-eight different structural features of the Georgia Coastal Plain are shown on a map and the bases of their identification and recognition are outlined. They are divided into tectonic framework features (the Okefenokee and Appalachicola Embayments with an intervening Central Georgia Uplift), folds (predominantly the Chattahoochee Anticline), and faults (most, if not all, normal). The framework appears to be both Cretaceous and Cenozoic in age, whereas the folding and faulting appear to be Cenozoic. One new feature, the Charlton High, is suggested from the absence of Oligocene rocks in the region of Charlton County. A striking southwest-northeast alignment of the features is evident as are certain specific geophysical trends such as gravity and magnetic anomaly alignments. Tension appears to have been a predominant source of energy for the faulting.

INTRODUCTION

The information for the accompanying map, Figure 1, was originally gathered for a structural map of the Coastal Plain of the United States being prepared by the Gulf Coast Association of Geological Societies. Since the scale of their map will not permit all of the features which are known to be included, it seems appropriate to publish the complete data for those who may be interested in these smaller features.

Sources

The map (Figure 1) is a compilation of information primarily taken from the originally-published version that included the names or the geographic definition of features or from later, often more detailed reports. In a few instances, minor revisions are supplied, largely to accommodate scale. The features are reproduced as closely as possible to the authors' original intent, both as to scale and levels of confidence, i. e., possible, probable or definite and named. One new name (Charlton High) is included for a feature which had been recognized earlier, but not named.

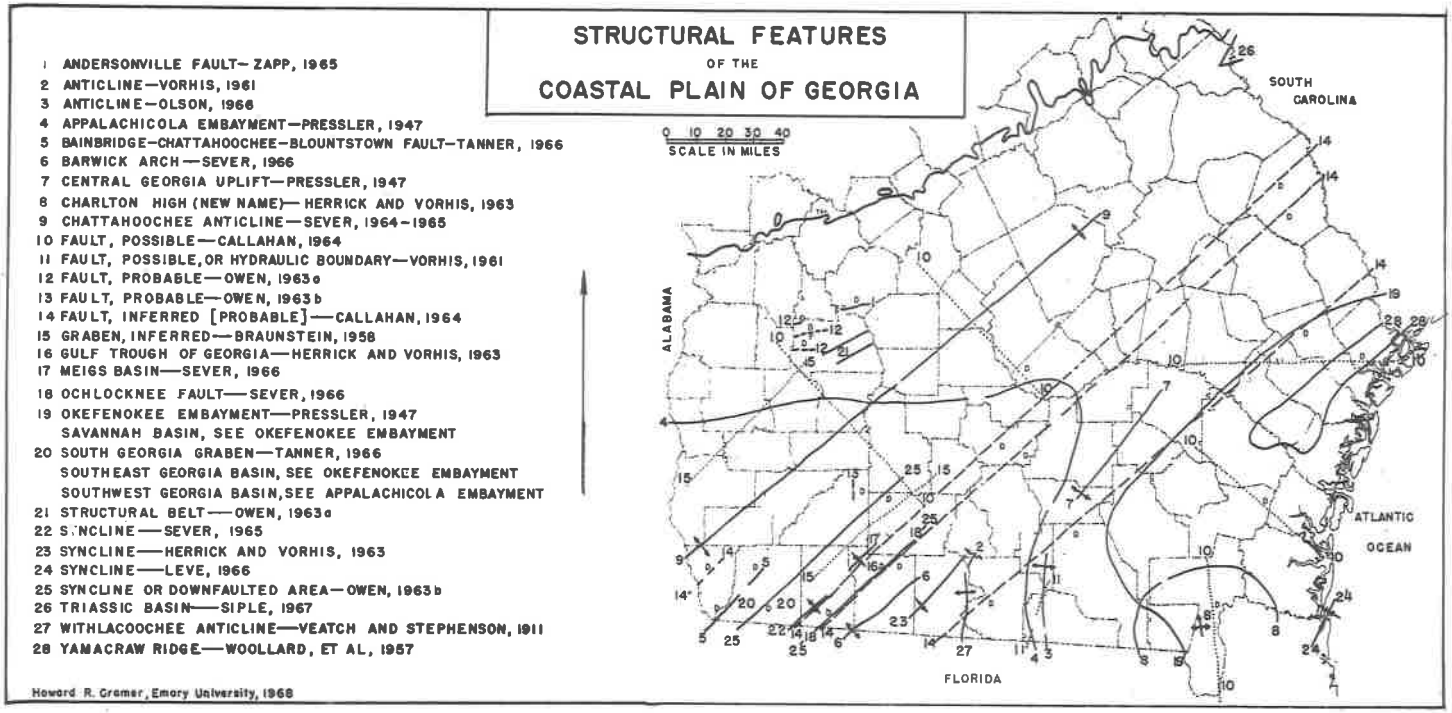

Figure 1. Structural features of the Coastal Plain of Georgia.

Acknowledgements

It is a pleasant obligation to note that many people have been generous with their time and information, not the least of whom are C. W. Sever, Jr., H. W. Straley, III and R. C. Vorhis.

TECTONIC FRAMEWORK OF THE GEORGIA COASTAL PLAIN

The Coastal Plain of Georgia is underlain, in general, by a wedge of sediments and rocks that thickens seaward. They are of at least Lower Cretaceous to Holocene in age. These rest upon a basement of crystalline rocks of uncertain age and upon rocks of Paleozoic and Triassic age. Comparatively little is known about the basement rocks and their structures because few wells have penetrated to them and a relatively small amount of detailed geophysical work has been carried out.

Because the basement rocks are essentially unknown, and since the definition of basement itself in Georgia is subject to discussion (Milton and Hurst, 1965), the crystalline and Paleozoic rocks and their structures are not included in this report except as where their influence can be detected in the structures in the overlying sedimentary materials.

Triassic Features

Triassic rocks underlie the Coastal Plain of southwestern Georgia (Richards, 1948; Applin, 1951) although little data were available upon which to base any structural interpretations. McKee and others (1959) interpreted the rocks as having come from shelf-type sediments which were thickening toward the southwest. Braunstein (1958) plotted inferred Triassic grabens (15, these numbers referring to the numbered features on Figure 1) on a small-scale map but he did not include his sources of evidence. Siple (1967) identified a Triassic basin (26) on the basis of lithology from a well core and from geophysical information. The dating of these structures as Triassic is presumably based upon the observation that the proposed boundary faults, while confining Triassic rocks, do not appear to offset the overlying Cretaceous rocks and also because such graben-like features are known elsewhere along the eastern coast of the United States.

Cretaceous and Cenozoic Features

The dominant framework features of the Georgia Coastal Plain are two great sedimentary basins with an accompanying high area between them. The Okeefenokee Embayment of the Atlantic Basin (19) was named by Pressler (1947) on the basis of the relatively thick

sedimentary section which had been found to exist in that part of Georgia. This same feature has been called the Southeast Georgia Embayment by Toulmin (1955) and the Atlantic Embayment of Georgia by Herrick and Vorhis (1963). The Appalachicola Embayment of the Gulf Basin was also named by Pressler. This same feature was called the Southwest Georgia Embayment by Murray (1961).

The high area between these two embayments, the Central Georgia Uplift (7) was named by Pressler (1947) who recognized it as a southeast-northwest striking ridge between the two flanking lower areas. The structure contour and isopachous maps of Herrick and Vorhis (1963) suggest that this feature would be better oriented with a southwest-northeast trend in order to accommodate sedimentary patterns. This latter orientation was also shown on the basement configuration map of Woollard and others (1957).

These three main features, the two sedimentary basins and the intervening Central Georgia Uplift, are geographically located on Figure 1 by the -4000 contour line of Woollard and others (1957). Their basement configuration was defined by the surface of marked seismic velocity change between the known sedimentary rocks and the basement below.

The embayments and the intervening high could be, according to Murray (1956), part of a larger system of southeast-northwest oriented lineaments that he recognized in the eastern United States. He noted that the Okeefenokee Embayment lies to the southeast of what he calls the Knoxville Salient in the Appalachian Mountains, and that the Peninsular Arch of Florida and the Central Georgia Uplift (with an implied northwest-southeast orientation) lay along a similarly-oriented lineament to the southeast of what he calls the Rome Recess in the Appalachian Mountains. This latter trend is noted by Hersey and others (1959) as part of a possibly much larger tectonic problem in which the arcuate trend of the crystalline rocks of the Piedmont of Georgia and neighboring states is analogized to the Japanese archipeligo of today and the Central Georgia Uplift-Peninsular Arch trend is analogized to the Ryukyu chain of today.

Actually, the two Georgia embayments and the intervening uplift were recognized early by geologists working on the Georgia Coastal Plain, but because of the paucity of data, no names or definitions were offered. For instance, Veatch and Stephenson (1911, p. 239) established the existence of the Okeefenokee Embayment when they noted a great sedimentary basin to the southeast, based upon changes in elevation of key horizons in the subsurface, but the lack of deep-well data prevented them from realizing the extent of this sedimentary basin. In 1923, Prettyman and Cave evaluated the state for its petroleum possibilities and outlined many of the structural features. They prepared a structure-contour map on a unit within the basal portion of the Miocene Alum Bluff Formation. Their map shows the influence, structurally, of what is now the northern part of the Peninsular Arch of Florida in the area

where it dies out in southern Georgia and also shows what are now called the Appalachicola and Okeefenokee Embayments. They suggested by their map that the intervening area (now the Central Georgia Uplift) trends northwest rather than northeast as it is now understood. Their map also shows other minor flexures which have been identified by later workers who had more data. Prettyman and Cave suggested no names, however.

The geological ages of these two embayments can be understood in part by an analysis of the isopachous and structural contour maps of Herrick and Vorhis (1963). The two embayments served as sediment traps and appear in the sedimentary record in the Cretaceous and Tertiary Periods. The Appalachicola Embayment first received a thickened section of sediments during the Lower Cretaceous (?) and during part of the Upper Cretaceous, although the deposition centers were different. Both the Okeefenokee and Appalachicola Embayments were serving as traps during the middle and upper Eocene, the Gulf Trough of Georgia (16) being the deposition center of the latter. Neither basin existed during the Oligocene, although the areas were receiving sediments. During the Miocene to Holocene interval, both embayments were again acting as basins though the volume of sediments is considerably reduced, as are the areas of the embayments. The Gulf Trough, however, remains a conspicuous feature.

Minor Framework Features

The Yamacraw Ridge (28) is a basement surface feature recognized and named by Woollard and others (1957) and according to the maps of Herrick and Vorhis (1963) appears to be influential on post-Tuscaloosa Cretaceous sedimentation but less so before and hardly at all afterwards. There is very little subsurface data from this part of the state, however, and it is difficult to draw meaningful conclusions. It is impossible to tell whether this ridge is a pre-Cretaceous feature upon which Coastal Plain sediments were deposited or whether it formed during the Cretaceous, or both.

The Charlton High (8) is a new name proposed herein for an area in Charlton County, Georgia, in which no Oligocene rocks are present. There is no evidence available whether this absence is due to a lack of Oligocene sedimentation caused by pre-Oligocene uplift or to a removal of Oligocene rocks in post-Oligocene, pre-Miocene time. The widespread blanket of Oligocene rocks over the Coastal Plain would make the latter possibility seem more likely.

Finally, a framework feature which has been hard to identify physically, the Okeefenokee Lineament of Thom (1959), trends roughly east-west across the southern end of the Georgia Coastal Plain. While Thom does not discuss the evidence for this feature, it appears to be related to the Ouachita structural trend toward the west. This feature cannot be shown on Figure 1, as Thom's map is very small-scaled and he gives no coordinates or geological reference points.

FOLDING

Upon the framework just outlined, folds and faults have been identified. Some of the first modern geologists to recognize that the Coastal Plain was not underlain by a gently-, seaward-dipping homocline were Spencer, who noted (1891) changes in the direction of the dip of the rocks, and Langdon (1891) who also noted reversals of dip in a section which he measured along the Chattahoochee River. These men offered no names or definitions, however.

Veatch and Stephenson (1911) were the first geologists to identify specific structural features and propose names. They recognized the Chattahoochee Anticline (9) and the Withlacoochee Anticline (27) from physiographic evidence alone. They found that the erosion patterns and drainage peculiarities of the Chattahoochee and Withlacoochee Rivers could best be explained as products of anticlinal flexures in the rocks. Sever (1964-1965), with much more data available, suggested that the orientation of the Chattahoochee Anticline be altered to a more northeast-southwest trend as shown rather than the north-south trend as Veatch and Stephenson would have had it. Sever gave a detailed resume of the history of the knowledge of this feature. Pressler (1947) called this feature the Decatur Arch.

The Chattahoochee Anticline was formed most probably during the early Miocene according to Sever (1964-1965) although Stephenson (1928) placed the dates of movement as late Tertiary and even early Quaternary based upon geomorphological evidence.

The Withlacoochee Anticline was elaborated upon by Olson (1966) who showed how it could be detected on the maps of Herrick and Vorhis and how it could be detected from lithological data which he had obtained. This structure had formed by the end of late Oligocene time.

Other smaller undulations in the Coastal Plain sedimentary rocks, most being within the Appalachicola Embayment, can be seen on the map; some have been identified by name. Most have been recognized from subsurface information although a few have surface expression, or are detectable from surface geology. Several had been recognized by Prettyman and Cave (1923), one of which, in Echols County (3), was later described and defined in more detail by Olson (1966).

The age of the folding in southwestern Georgia appears to be Tertiary, although different episodes of folding seem to be indicated; some is as late as Miocene (Sever, 1966).

Finally, it should be noted that the Central Georgia Uplift (7) and the Charlton High (8) are shown on Figure 1 as anticlines although their real tectonic origin is uncertain. Not enough evidence is available to determine whether they were ever positive elements or simply residual high areas from the foundering of the areas adjacent to them.

FAULTING

Faults on the Georgia Coastal Plain are, by and large, more nebulous than the other features. Most, if not all, appear to be high-angled, and those which have been clearly identified are normal. Most have been recognized on the basis of vertical offset of key horizons, and fault planes have never been seen. Several have been postulated on the basis of dip irregularities and have been called structural belts (21) or downfaulted areas (25), as little evidence of their actual nature exists.

Several rather large faults (10, 11, 14) have been postulated on the basis of hydrologic peculiarities. This criterion was especially significant in identifying those which trend entirely across the state (14) and those which are normal to them (10). These were proposed by Callahan (1964) from an evaluation of the distribution of large springs in the state, from their discharge, and from peculiar patterns on the piezometric-surface map of the Coastal Plain, which could best be explained by offsetting of aquifers.

The Gulf Trough of Georgia (16) was identified within the Appalachicola Embayment by Herrick and Vorhis (1963) from information gleaned from isopachous and structure contour maps prepared from subsurface data. This feature is distinctly linear and more sharply defined than the surrounding folds so that it would seem to be better classed as a fault structure although they do not indicate which is more likely. The Gulf Trough of Georgia was recognized but not named by Spencer (1891) who, on the basis of exposures of Eocene rocks in southern Georgia and northern Florida, concluded that a structural trough filled with Miocene sedimentary rocks lay between the Eocene outcrops.

The Gulf Trough of Georgia is further substantiated as a possible fault feature because it appears to be coincident with the South Georgia Graben (20) proposed by Tanner (1966). This graben, according to Tanner, attracted one of the rivers on the Appalachicola River system during the Miocene and possibly even later (Tanner, 1955). The evaluation of the cross-bedding indicates that the sedimentation was estuarine and that the orientation of the body of water was similar to the orientation of the Gulf Trough and the South Georgia Graben. Tanner (1966) indicates that the river system was in existence during the Pliocene also, at least farther to the south. This graben would appear to be bounded on the southeast by the Ochlochnee Fault (18) and on the northwest by the syncline or downfaulted area (25).

It is difficult to date with any certainty any of the faulting on the Georgia Coastal Plain, as all of the faults cut Tertiary rocks with no minimum age to be found. Some at least, the Ochlochnee (18) in particular, are at least Miocene or post-Miocene, and the Chattahoochee-Bainbridge-Blountstown Fault (5), identified on the basis of vertical offsetting of erosion surfaces, may be as young as Pliocene.

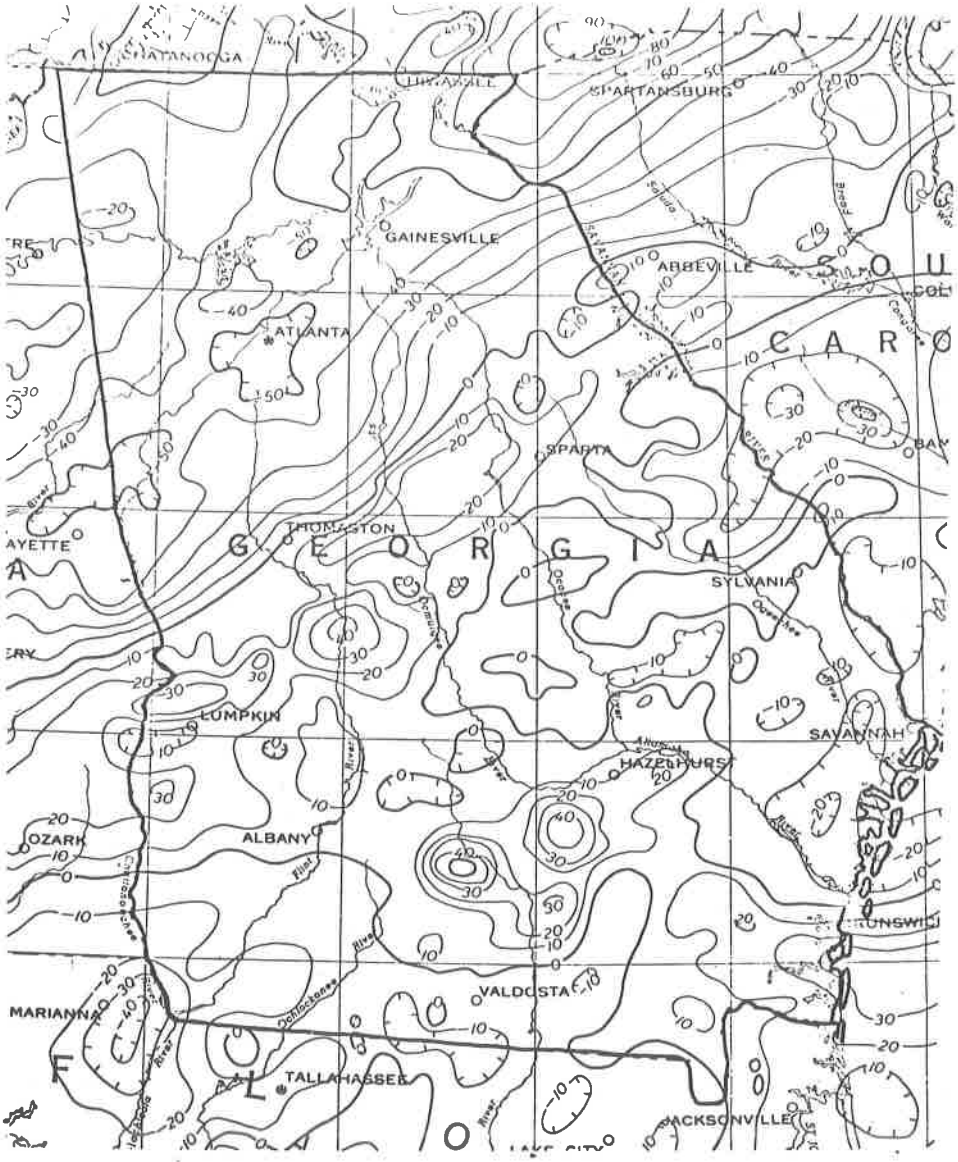

Figure 2. Bouguer gravity anomaly map of Georgia, from Bouguer gravity anomaly map of the United States, Amer. Geophysical Union, 1964.

ADDITIONAL INFORMATION

Some additional information may be of some value to the reader in order to view these structures of the Georgia Coastal Plain as part

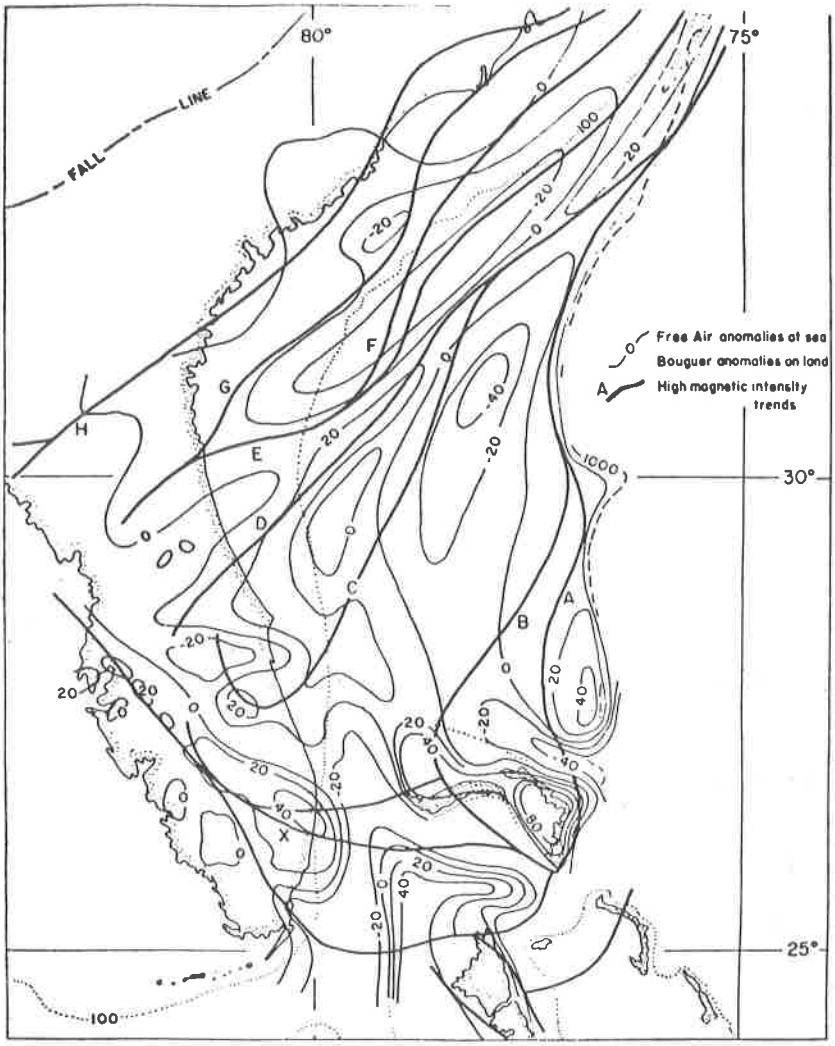

Figure 3. Magnetic high-intensity trends and gravity anomalies, Blake Plateau and southeastern United States, from Drake, 1963, p. 5268.

of a larger panorama. For instance, the Bouguer gravity anomaly map of the United States (Amer. Geophysical Union, 1964), of which the Georgia portion is reproduced as Figure 2, indicates some southwest-northeast lineaments of anomalies, although admittedly somewhat less than unequivocal.

No magnetic map of the Georgia Coastal Plain has been published, although the magnetic map of Florida (King, 1959) includes part of southern Georgia. The map of magnetic high-intensity trends in the southeastern United States (Drake and others, 1963) includes parts of Georgia and is reproduced here as Figure 3 for the convenience of the

reader.

A seismic map of the configuration of the basement surface was published by Woollard and others (1957).

INTERPRETATIONS

Since this work is intended primarily as a compilation of the location of the major structural features with a bit of explanation as regards their recognition, and because the Obscurocity Quotient*, here defined as

$$ObsQ=\frac{unknown}{known},$$

is very high, the writer is reluctant to do more than elaborate upon some of the obvious aspects.

(1) Even the casual reader cannot help but notice the pronounced northeast-southwest trend of most of the features, and especially the larger ones. These trend roughly parallel with some of the larger structural features of the Piedmont and Appalachian Mountains, such as the Pine Mountain Belt, bounded by the Towaliga and Goat Rock Faults; the Brevard Zone, and even the general trend of the Piedmont and Appalachian Mountains themselves. As a matter of fact, these trends parallel the eastern coast of the United States north of Florida.

(2) The Bouguer gravity anomaly map of Georgia (Figure 2) shows similarly-oriented trends, although admittedly not as pronounced.

(3) The magnetic-anomaly trend map of Drake and others (1963) shows northeast-southwest oriented trends (Figure 3).

(4) The density of structural features in the Appalachicola Embayment may be actually greater than in other areas as indicated, or it may be simply a reflection of the availability of information. In this area of thick sedimentary rocks, there has been more interest by petroleum companies and also, probably coincidentally, clays have spurred geologic investigation. In either case, it is evident that structural features on the Georgia Coastal Plain are more numerous than one would generally be inclined to think.

(5) While little is known of the regional tectonic nature of southern Georgia, it does appear that tension has played an important part in the creation of the structures. The map expression of the faults, their apparently straight traces, and in some cases actual observation of the deformation patterns (such as vertical displacements) suggest that much of the faulting is normal; some may be related to the Chattahoochee Anticline (Sever, 1964-1965).

* the reciprocal naturally is the Obvioucity Quotient,

$$ObvQ=\frac{1}{ObsQ}$$

(6) The Triassic grabens, actual and inferred, would be a product of tension.

REFERENCES CITED

American Geophysical Union and U. S. Geological Survey, 1964, Bouguer gravity anomaly map of the United States. Scale, 1 inch to approx. 40 miles.

Applin, P. L., 1951, Preliminary report on buried pre-Mesozoic rocks in Florida and adjacent states: U. S. Geol. Survey Circ. 91, 28 p.

Braunstein, Jules, 1958, Habitat of oil in eastern Gulf Coast, in Habitat of oil--a symposium (L. G. Weeks, ed.): Tulsa, Okla., Amer. Assoc. Petroleum Geologists, p. 511-522; with slightly different title: World Oil, v. 146, no. 7, p. 133-139; 1959, Ga. Mineral Newsletter, v. 12, p. 12-16.

Callahan, J. T., 1964, The yield of sedimentary aquifers of the Coastal Plain, southeast River basins: U. S. Geol. Survey Water-Supply Paper 1669-W, 56 p.

Drake, C. L., Heirtzler, J., and Hirshman, J., 1963, Magnetic anomalies off eastern North America: Jour. Geophysical Research, v. 68, p. 5259-5275.

Herrick, S. M., and Vorhis, R. C., 1963, Subsurface geology of the Georgia Coastal Plain: Ga. Geol. Survey Inf. Circ. 25, 80 p.

Hersey, J. B., Bunce, E. T., Wyrick, R. F., and Dietz, F. T., 1959, Geophysical investigations of the continental margin between Cape Henry, Virginia, and Jacksonville, Florida: Geol. Soc. America Bull., v. 70, p. 437-466.

King, E. R., 1959, Regional magnetic map of Florida: Amer. Assoc. Petroleum Geologists Bull., v. 43, p. 2844-2854.

Langdon, D. W., Jr., 1891, Geological section along the Chattahoochee River from Columbus to Alum Bluff: Ga. Geol. Survey Prog. Rept. 1, 1890-1891, p. 90-97.

Leve, G. W., 1966, Ground water in Duval and Nassau Counties, Florida: Fla. Geol. Survey Rept. Inv. 43, 91 p.

McKee, E. D., Oriel, S. S., Ketner, K. B., MacLachlan, M. E., Goldsmith, J. W., Maclachlan, J. E., and Mudge, M. R., 1959, Paleotectonic maps of the Triassic System: U. S. Geol. Survey Mic. Geol. Inv. Map I-300, 33 p.

Milton, Charles, and Hurst, V. J., 1965, Subsurface "basement" rocks of Georgia: Ga. Geol. Survey Bull. 76, 56 p.

Murray, G. E., 1956, Relationships of Paleozoic structures to large anomalies of coastal element of eastern North America: Gulf Coast Assoc. Geol. Soc. Trans., v. 6, p. 13-24.

_____, 1961, Geology of the Atlantic and Gulf Coastal Province of North America: New York, Harper, 692 p.

Olson, N. K., 1966, Phosphorite exploration in portions of Lowndes, Echols, Clinch, and Charlton Counties, Georgia: Ga. Geol. Survey South Georgia Minerals Program Prog. Rept. 4, 116 p.

Owen, Vaux, Jr., 1963a, Ground-water resources of Lee and Sumter Counties, southwest Georgia: U. S. Geol. Survey Water-Supply Paper 1166, 70 p.

_____, 1963b, Geology and ground-water resources of Mitchell County, Georgia: Ga. Geol. Survey Inf. Circ. 24, 40 p.

Pressler, E. D., 1947, Geology and occurrence of oil in Florida: Amer. Assoc. Petroleum Geologists Bull., v. 31, p. 1851-1862.

Prettyman, T. M., and Cave, H. S., 1923, Petroleum and natural gas possibilities in Georgia: Ga. Geol. Survey Bull. 40, 167 p.

Richards, H. G., 1948, Studies on the subsurface geology and paleontology of the Atlantic Coastal Plain: Acad. Nat. Science Philadelphia Proc., v. 100, p. 39-76.

Sever, C. W., Jr., 1964-65, The Chattahoochee Anticline in Georgia: Ga. Mineral Newsletter, v. 17, p. 39-43.

_____, 1965, Ground-water resources and geology of Seminole, Decatur, and Grady Counties, Georgia: U. S. Geol. Survey Water-Supply Paper 1809-Q, 30 p.

_____, 1966, Miocene structural movements in Thomas County, Georgia: U. S. Geol. Survey Prof. Paper 550-C, p. 12-16.

Siple, G. E., 1967, Geology and ground water of the Savannah River Plant and vicinity, South Carolina: U. S. Geol. Survey Water-Supply Paper 1841, 113 p.

Spencer, J. W. W., 1918, A general or preliminary geological report on southwest Georgia...: Ga. Geol. Survey Prog. Rept. 1, 1890-1891, p. 11-90.

Stephenson, L. W., 1928, Structural features of the Atlantic and Gulf Coastal Plain: Geol. Soc. America Bull., v. 39, p. 887-900.

Tanner, W. F., 1955, Paleogeographic reconstruction from cross-bedding studies: Amer. Assoc. Petroleum Geologists Bull., v. 39, p. 2471-2483.

Thom, W. T., Jr., 1959, Tectonic sketch map of North America..., Scale, 1 inch to 10 million inches: Red Lodge, Montana, Yellowstone-Bighorn Research Association.

Toulmin, L. D., Jr., 1955, Cenozoic geology of southeastern Alabama, Florida, and Georgia: Amer. Assoc. Petroleum Geologists Bull., v. 39, p. 207-235.

Veatch, J. O., and Stephenson, L. W., 1911, Preliminary report on tne geology of the Coastal Plain of Georgia: Ga. Geol. Survey Bull. 26, 466 p.

Vorhis, R. C., 1961, A hydrogeologic reconnaissance of reservoir possibilities in northern Lowndes County, Georgia: Ga. Mineral Newsletter, v. 14, p. 123-129.

Woollard, G. P., Bonini, W. E., and Meyer, R. P., 1957, A seismic refraction study of the sub-surface geology of the Atlantic

Coastal Plain and continental shelf between Virginia and Florida: Univ. Wisconsin Dept. Geology and Geophysics, 128 p.

Zapp, A. D., 1965, Bauxite deposits of the Andersonville district, Georgia: U. S. Geol. Survey Bull. 1199-G, 37 p.